AD-A039 641 PENNSYLVANIA STATE UNIV UNIVERSITY PARK APPLIED RESE--ETC F/G 13/11
TEST RESULTS FROM A PROGRAM DETERMINING THE PERFORMANCE OF A VA--ETC(U)
FEB 77 A YOCUM N00017-73-C-1418
UNCLASSIFIED TM-77-34 NL

| OF |
AD A039641

END
DATE FILMED
6-77

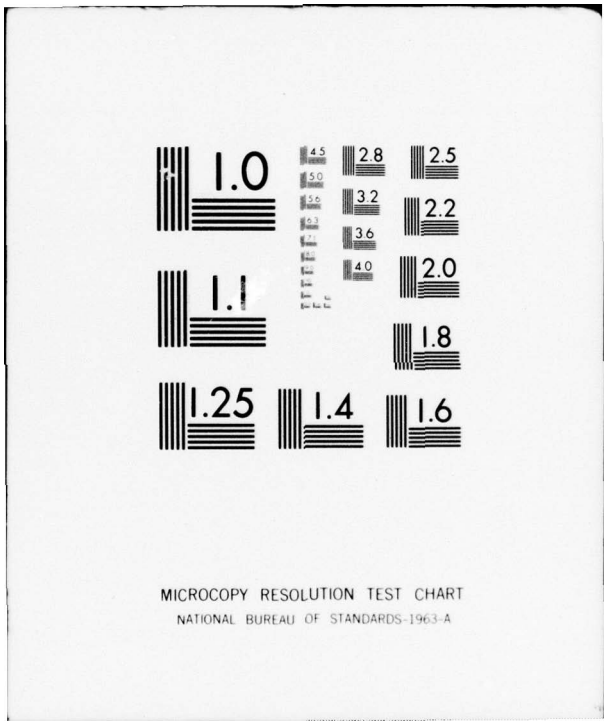
1.0
1.1
1.25
1.4
1.6
1.8
2.0
2.2
2.5
2.8
3.2
3.6
4.0
4.5
5.0
5.6
6.3
MICROCOPY RESOLUTION TEST CHART
NATIONAL BUREAU OF STANDARDS-1963-A

12

TEST RESULTS FROM A PROGRAM DETERMINING THE PERFORMANCE OF A VANED VOLUTE TO BE USED AS A DOUBLE SUCTION PUMP INLET

A. Yocum

Technical Memorandum
File No. TM 77-34
February 8, 1977
Contract No. N00017-73-C-1418

Copy No. 30

The Pennsylvania State University
APPLIED RESEARCH LABORATORY
Post Office Box 30
State College, PA 16801

NAVY DEPARTMENT

NAVAL SEA SYSTEMS COMMAND

SECURITY CLASSIFICATION OF THIS PAGE (When Data Entered)

REPORT DOCUMENTATION PAGE

READ INSTRUCTIONS BEFORE COMPLETING FORM

1. REPORT NUMBER: TM-77-34	2. GOVT ACCESSION NO. (9) Technical memo.
3. RECIPIENT'S CATALOG NUMBER	
4. TITLE (and Subtitle): TEST RESULTS FROM A PROGRAM DETERMINING THE PERFORMANCE OF A VANED VOLUTE TO BE USED AS A DOUBLE SUCTION PUMP INLET.	5. TYPE OF REPORT & PERIOD COVERED
	6. PERFORMING ORG. REPORT NUMBER
7. AUTHOR(s): A. Yocum (11) 8 Feb 77	8. CONTRACT OR GRANT NUMBER(s): N00017-73-C-1418
9. PERFORMING ORGANIZATION NAME AND ADDRESS: Applied Research Laboratory, P. O. Box 30, State College, PA 16801	10. PROGRAM ELEMENT, PROJECT, TASK AREA & WORK UNIT NUMBERS
11. CONTROLLING OFFICE NAME AND ADDRESS: Naval Sea Systems Command, Washington, D.C. 20362 (12) 62p.	12. REPORT DATE: February 8, 1977 13. NUMBER OF PAGES: 61
14. MONITORING AGENCY NAME & ADDRESS (if different from Controlling Office)	15. SECURITY CLASS. (of this report): UNCLASSIFIED 15a. DECLASSIFICATION/DOWNGRADING SCHEDULE

16. DISTRIBUTION STATEMENT (of this Report)

Approved for public release. Distribution limited.
Per NAVSEA - April 14, 1977

17. DISTRIBUTION STATEMENT (of the abstract entered in Block 20, if different from Report)

18. SUPPLEMENTARY NOTES

19. KEY WORDS (Continue on reverse side if necessary and identify by block number)

Suction pump
Vaned inlet volute
Flow simulation

20. ABSTRACT (Continue on reverse side if necessary and identify by block number)

This report describes the test program for determining the performance of a new type of vaned inlet volute for a double suction pump. The volute was intended for use in a new high speed planing craft waterjet propulsion system currently under development by DTNSRDC. A short description of the volute and the remaining test apparatus, which simulates the flow in the entrance duct of the craft, is included. Results from measurements at various stations throughout the system are presented and discussed, and recommendations for improvements and future studies are made.

DD FORM 1 JAN 73 1473 EDITION OF 1 NOV 65 IS OBSOLETE

UNCLASSIFIED
SECURITY CLASSIFICATION OF THIS PAGE (When Data Entered)

391 00.7

Abstract: This report describes the test program for determining the performance of a new type of vaned inlet volute for a double suction pump. The volute was intended for use in a new high speed planing craft waterjet propulsion system currently under development by DTNSRDC. A short description of the volute and the remaining test apparatus, which simulates the flow in the entrance duct of the craft, is included. Results from measurements at various stations throughout the system are presented and discussed, and recommendations for improvements and future studies are made.

Acknowledgments: This work was sponsord by DTNSRDC, Annapolis, MD.

Table of Contents

List of Figures

February 8, 1977
AY:tms

Nomenclature

A	Cross-sectional area of the flow duct
C_{pr}	Pressure recovery coefficient $(P_2 - P_1)/\frac{1}{2}\rho V_1^2$
C_{ps}	Dimensionless static pressure $(P_s - P_{atm})/\frac{1}{2}\rho V_\infty^2$
C_{pT}	Dimensionless total pressure $(P_T - P_{atm})/\frac{1}{2}\rho V_\infty^2$
d	Distance measured from the bottom of the duct at the throat
g	acceleration of gravity
H	Height of the duct at the diffuser exit
h	Height of the duct at the throat
h_L	Head loss
k_L	Head loss coefficient defined by eq. (7)
P_{atm}	Atmospheric pressure
P_s	Static pressure
P_T	Total pressure
r	Radial coordinate used in the test section
V	Velocity
V_1	Average velocity at the diffuser inlet
V_∞	Maximum velocity in the throat
W	Width of the duct at the diffuser exit
X	Vertical coordinate at the diffuser exit
Y	Horizontal coordinate at the diffuser exit
Z	Axial coordinate

Greek Symbols

η_p	Pressure recovery efficiency defined by eq. (5)
ρ	Mass density of the fluid
θ	Angular coordinate used in the test section

Subscripts

r	Corresponds with the r coordinate
θ	Corresponds with the θ coordinate
x	Corresponds with the x coordinate
y	Corresponds with the y coordinate
z	Corresponds with the z corrdinate
1	Diffuser entrance (throat)
2	Diffuser exit

Introduction

The purpose of this report is to describe the tests made to determine the performance of a new type of vaned inlet volute for a double suction pump. This research was conducted for the Naval Ship Research and Development Center of Annapolis, MD as part of the advanced development program for waterjet propulsion systems. The design of the inlet under present consideration was initiated to try to eliminate some of the typical problems encountered with conventional inlets.

Conventional inlets are constructed such that the inlet flow is divided into two streams which flow around both sides of the axis of the machine. At the rear of the machine, where the flows would converge, a splitter vane is located which separates the two streams and directs them into the eye of the impeller. One problem resulting from this type of arrangement is due to the fact that the flows on opposite sides of the axis have circumferential components of velocity which are in opposite directions. This fact, obviously, makes it impossible for the impeller vanes to be operating on design, except at the circumferential location where the local swirl is equal to the mean swirl for which the impeller is designed. As a consequence of the impeller vanes operating off design at most locations, the losses in the impeller will be increased and the possibility of cavitation occuring is greater.

Besides the non-uniform swirl, the splitter vane used with a conventional inlet causes additional performance degradation. This is because the splitter vane will shed a large wake into the flow, which is seen by the rotor as a flow distortion or non-uniformity. This will result in the usual problems associated with distorted flow, such as unsteady blade forces, vibration, noise, poorer performance and poorer cavitation resistance.

To avoid the non-uniform swirl and to eliminate the splitter vane which creates a flow distortion, it is advantageous to use an inlet volute to supply the flow to the eye of the impeller. A plain volute, however, also creates problems with severe limitations. As the fluid nears the axis of the machine, the radius is decreasing and the circumferential component of velocity must increase to conserve angular momentum. This means that near the eye of the impeller and especially in the hub region, extremely large values of circumferential velocity will exist. The large amount of swirl at the inlet makes it very difficult to obtain the desired head rise, since less turning can be put into the flow. The large circumferential velocity component also decreases the static pressure and thus lowers the machines resistance to cavitation. To overcome these problems, but still retain the advantages of a volute, it was suggested that a volute be designed with vanes near the hub which would remove the swirl. It was intended with this type of configuration, that the volute would evenly distribute the flow around the circumference, and the vanes after removing the swirl would thus provide a uniform axial flow to the impeller.

Due to the complexity of the flow, accurate performance predictions could not be made. Therefore, in order to evaluate the performance of a vaned volute, it was necessary to design and build a system of which the performance could be measured. A photograph of the volute and vane

system built and tested is shown in Figure 1. The volute has the shape of an Archimedean spiral and the vanes are circular arcs. A large fillet is located on the side opposite the exit, to help direct the flow into the axial direction.

The performance criteria of concern are the uniformity of the exit flow, the amount of remaining swirl, and the pressure losses through the system. These data were obtained by taking velocity and pressure surveys at various stations throughout the system.

Facility Description

The facility for testing the volute was designed with the purpose of simulating the actual flow conditions which would exist if the volute were installed in the proposed planing craft. This required incorporating into the system the diffusing transition section which connects the approximately square volute inlet to the wide narrow entrance. The inclusion of this component was necessary since its performance was unknown, and also since there can be an interaction between the diffuser and the volute. These and the remaining components of the system are shown in the photographs of Figures 2 and 3. A schematic of the facility and the instrumentation is also provided in Figure 4, with the different components labeled for identification.

Smooth entrance to the system is provided by the bellmouth entrance shown in the photographs and the schematic. The section immediately downstream of the entrance is provided to produce a velocity profile similar to the profile in the entrance duct of the craft. The velocity profile is developed by stretching wires of predetermined diameter across the inlet. A settling section downstream of the wires then allows the wakes from each individual wire to mix out forming a smooth profile of the desired shape. The design shape of the profile was provided by NSRDC based on their estimates of velocity profile resulting from removing the fluid from the bottom of the craft through a flush mounted inlet. The non-uniformity of the profile is the result of removing fluid from the boundary layer on the bottom of the craft.

The inlet, the wires, and the settling section are provided simply to simulate the velocity profile which would enter the downstream components of the real system. They themselves, do not represent components of a real water jet pumping system, as do the remaining three components, the diffuser, the volute and the test section. At the plane designated as the throat in the schematic, the components representing the real system begin. Here the channel begins to diverge and diffuse the flow. The throat is the first measuring station and data obtained here defines the inlet velocity profile and will serve as a reference for the pressure losses throughout the remainder of the system.

A short distance downstream of the throat, the flow is divided between three separate channels. The center channel is the one leading to the volute and is the only one under consideration. The two side channels are provided so that the flow entering the center channel simulates the flow which would be entering, if there was a wide row of diffusers and volutes, as proposed for the actual planing craft.

The center channel, as previously mentioned, must serve a dual purpose. In addition to diffusing the flow, it must also provide a transition from the wide narrow inlet to the volute inlet shape. It is very important to diffuse the flow in order to improve the cavitation performance of the pump. However, due to its dual purpose, proper diffuser design cannot be followed, and it is therefore also important to evaluate the performance of this component of the system. Velocity and pressure measurements at the diffuser exit (or volute inlet) will identify any separation which has occurred, allow the efficiency of the diffusion process to be determined, define the velocity profile entering the volute, and provide pressure loss data so that the performance of the volute can be evaluated separately.

The volute is the next component of the system. No pressure or velocity measurements were made in the volute itself, but a plexiglass cover allows visual observation of a tuft on a probe to determine the flow patterns. In the photograph of Figure 1, the plexiglass cover has been removed clearly showing the inner areas which can be seen through the cover.

The section following the volute is designated as the test section in the schematic, since it is here where the performance of the volute is evaluated. This section represents the eye of the impeller and has an annular shape with a 3.0 inch diameter hub and a 7.5 inches diameter outer casing. The outer casing is free to rotate and has angular locations marked every 2 degrees, in order that circumferential surveys of the flow can be conducted. The axial location of the probe in the circumferential surveys was 1.5 inches downstream of the vanes trailing edges. It would have been preferred to locate the probe one span length (2.25 inches) downstream, since this distance represents the average distance to the impeller for commercial pumps. However, spatial limitations required that the measuring station be moved forward to allow clearance when rotating the casing and probe.

The remainder of the air system consists of flexible hose or stove pipe connections, butterfly valves, and two Buffalo Forge Exhausters. One side channel and the center channel are connected to the 2000 CFM exhausher. The other side channel is connected to the 1200 CFM exhauster. Butterfly valves arranged as shown in the schematic allow balancing and bypassing the flow to obtain an even flow distribution in the inlet section.

Instrumentation

The instrumentation for the various tests conducted is also shown schematically in Figure 4. The first pieces of instrumentation necessary, were the wedge probes which were used to align the flow in the airlet. As shown in the figure, these probes were located just upstream of the channel dividers and were connected to two U-tube manometers. The two manometers were inclined at approximately a 24° angle to increase their sensitivity. With the wedge probes pointed directly forward, aligning the flow required balancing the pressures from the two side holes of the probes, with the balanced condition indicated by equal fluid columns in the manometers. Proper adjustment of the flow was obtained through the butterfly control valves. During the course of a test, the manometers were checked periodically to assure proper flow alignment was being maintained.

The remainder of all pressure measurements were made with a single differential pressure transducer, through the use of a scanivalve. At the throat, 13 readings were taken at the beginning of each test, since these data were used as a reference. Four static pressure wall taps are located at the throat, two on the top and two on the bottom. Since the streamline curvature is small at this location, the top and bottom taps read approximately the same values. For the small difference that does exist, a linear variation of the static pressure across the section is assumed.

A nine tube total pressure rake is also located at the throat. This rake is used to establish the velocity profile entering the diffuser and determine the average total pressure of the flow. In the 2.5 inch section, the nine tubes equally spaced provide measurements every .25 inches. The rake is normally located at equal distances between the two walls, however the rake can be shimmed .125 inch to align the tubes with the upstream wires and thus measure if any wakes from the wires still exist.

The remainder of the surveys conducted were made with a United Sensor five hole probe, type DA-125-12-F-10-CD, used in the non-nulling mode. Horizontal and vertical surveys were conducted at the diffuser exit, and circumferential surveys at three radial locations were performed in the test section. However, before going into the description of these measurements, it is advantageous to give a brief description of the probe's characteristics and the calibrations necessary for its use in the non-nulling mode.

The reason a five hole probe was selected for these measurements is that this type of probe enables the total pressure, static pressure and the three components of velocity to be determined. The ability to resolve the velocity into its three components was considered an important asset in this study, since the radial and circumferential components of velocity in the test section were expected to be significant. The five hole probe is also capable of measuring the static pressure more accurately than other types of probes, since it can account for the direction of the flow.

The calibration of a five hole probe can require a considerable amount of time. However, data for the probe used had been obtained previously as part of another program. The calibration technique for this probe consisted of placing the probe in a known uniform velocity field and varying the pitch and yaw angle between the range of $\pm 30°$. At each angular location, the five pressures from the probe as well as the known total and static pressure of the flow were recorded. From these data, four pressure coefficients, a yaw coefficient, pitch coefficient, total pressure coefficient and a static pressure coefficient are defined. These coefficients, which are a function of the yaw and pitch angle, completely describe the probe's response to the flow.

With the above information known, when the probe is placed in an unknown flow, the yaw and pitch coefficients are once again calculated, but through the use of the calibration data the yaw and pitch angles of the unknown flow can now be determined. After the two angles are known, the total and static pressure coefficients are interpolated from the calibration data and the two pressures can then be calculated. The velocity is calculated with the Bernoulli equation and then broken into its components using the known angles.

One disadvantage of a five hole probe is that the calibration curves are usually weakly dependent on velocity, or if expressed non-dimensionally, Reynolds number. To investigate this effect, calibrations were conducted over a range of Reynolds numbers. These data revealed that for the range tested, only the static pressure coefficient was slightly affected. These data were used however, for calculating correction curves based on the average static pressure coefficient for the range of Reynolds numbers the probe would experience.

The five hole probe used in this study also has available calibration data examining the interference effect caused by the proximity of a wall. This type of interference is not unique with five hole probes, but exist for all probes when they are near enough to a wall, such that the streamlines around the probe are altered. Since the distance to the wall is known, it was also possible to incorporate wall-proximity data into the data reduction program and correct for the wall interference effect. Similar to the Reynolds number effect, only the static pressure coefficient needed to be corrected.

It may seem that the preceeding corrections limit the usefulness of a five hole probe due to the required amount of data and complexity of the data reduction program. However, it should be mentioned that the error in the calculated velocity resulting from neglecting the Reynolds number and wall proximity effects would only be a few percent. Therefore, these corrections could be eliminated without serious effect. However, since the data were available, they were used in this study.

The first station where measurements were made with the five hole probe was at the volute inlet. As previously mentioned, both vertical and horizontal traverses of the flow were made. Since the area ratio of the throat to the volute inlet is 1.6, the overall process between the two sections is a diffusion process, which could result in flow separation. However, the verical walls are converging and the horizontal walls are diverging. Under these flow conditions, it was felt to be necessary to survey the flow in both the vertical and horizontal directions in order to locate any separation zones and define properly to the velocity profile.

A commercially available United Sensor traversing device was used for locating the probe in the surveys at the volute inlet. This device had a vernier scale which allowed accurate placement of the probe within one one-hundredth of an inch. Measurements were made, starting with the probe tip touching the far wall and then moving the probe in .25 inch increments. When measurements were being made near the hole through which the probe entered, for all but the first run, the gap was sealed with wax to eliminate any effects caused by leakage.

The final station where measurements were made was in the test section, 1.5 inches downstream of the vanes. Here, circumferential surveys were conducted at locations 1/4, 1/2, and 3/4 of the distance across the annulus. These surveys were conducted with 6° increments for the entire 360°. Surveys over the full circumferential extent were necessary since it could not be assumed that any vane channels would operate similarly, due to their different positions around the volute. The 6° increments provide 10 measurements per vane channel which was adequate to accurately describe the flow field.

Results

The data for the various tests conducted are presented in this section. Starting with the data taken at the throat, Figure 5 is a plot of the dimensionless velocity and pressure versus the dimensionless distance from the bottom of the section. A sketch is included in the figure defining the coordinates. The results presented in Figure 5 were obtained from two different tests, one with the total pressure rake centrally located in the duct, and one with the rake offset .125 inches. These results indicate that no wakes from the wires remain, and a smooth velocity profile has been obtained. In Figure 6, data from the same tests are presented with the velocity non-dimensionalized by the mean velocity, comparing the profile obtained experimentally with the design data. Very good agreement is obtained in the low velocity region of the profile. In the higher velocity region, the two sets of data begin to diverge, but the results are still fairly good. A more accurate simulation of the velocity profile could be obtained by using the available data and modifying the diameter or the number of wires used. However the results seem adequate for the initial tests conducted.

The data from the flow surveys at the volute inlet are presented in Figures A.1 through A.12 of Appendix A. In these figures, the three dimensionless velocity components and the dimensionless total and static pressures are plotted as a function of location, for each of the three vertical and horizontal traverses. Figure 7, which is a schematic of the volute inlet, is provided to define the coordinate system used in presenting these data and it also shows the locations of the traverses.

The data measured at the volute inlet as shown by the figures, exhibit a significant amount of scatter. This scatter is probably due to the high turbulence level caused by the upstream wires which generate the inlet velocity profile. For both the horizontal and vertical traverses, the component of velocity parallel to the axis of the probe possesses the most scatter. The reason that the scatter appears primarily in this particular component of velocity is probably due to the geometry of the sensing element of this type of probe. The holes for sensing the component of velocity parallel to the axis of the probe are located on surfaces perpendicular to the axis. This arrangement results in the probe being extremely sensitive to fluctuations in this component. Several traverses were made in both directions, however, to verify the data and through averaging eliminate some of the scatter.

The first two horizontal and vertical traverses were conducted with the upstream total pressure rake installed. Subsequent examination of the horizontal traverse data, revealed that a significant wake is shed by the total pressure rake. To correct this error, one additional traverse in each direction was conducted with the rake removed. After eliminating the effect caused by the wake, the horizontal traverses indicate a uniform profile exists and no separation has occurred in this plane.

As just mentioned, the first two vertical traverses were also conducted in the wake of the total pressure rake. Therefore, it was necessary to use the third traverse to correct V_z/V_∞ and C_{pT} in the first two tests. After corrections were made, all three traverses could then be averaged to eliminate some of the scatter and obtain more meaningful results. The averaged data are presented in Figures 8 and 9 along with some predicted results obtained using several different methods. These predictions were made with the hope of explaining the shape of the profiles at the volute inlet and will be discussed later. For now, several other observations are necessary.

The dimensionless velocities plotted in Figure 8 are plotted with the same scale as the velocity in the throat, which was presented in Figure 5. Comparison of these two figures, reveals that the velocity gradient has been decreased by the diffusion process. Similarly, comparison of the total pressure at the volute inlet with the total pressure distribution in the throat indicates the total pressure gradient has also been decreased. This behavior is favorable since the reverse behavior could possibly result in flow separation and higher losses. As the data shows, no separation has occurred in the vertical plane where measurements were made.

Referring again to Figure 8, the horizontal component of velocity (V_y) is shown to be approximately zero, as would be expected. The average value of the vertical component, however, despite the scatter, is seen to be positive. A similar conclusion is drawn by examining Figures A.7 through A.9. Although this conclusion may seem peculiar, it is consistent with the fact that for the velocity and total pressure gradients to decrease, some of the higher energy fluid in the lower region of channel must be convected upward. Therefore the vertical velocity component as indicated in the figure is due to the flow redistribution taking place.

The final results to be presented, were obtained from measurements made in the test section just downstream of the volute exit. These data are presented in Figures B.1 through B.15 which appear in Appendix B. In these figures the dimensionless axial, radial, and circumferential components of velocity, and the dimensionless total and static pressure are plotted as functions of circumferential location for three different radii. The circumferential component of velocity and the circumferential location are positive in the clockwise direction when looking toward the volute from the test section. This direction corresponds to the direction of the flow swirl put into the flow by the volute. The location of the 0° position is approximately 10° clockwise from the vertical position and was selected such that the measurement made at 0° and the mean radius would be directly aligned with a vane. However, due to the mean swirl which still remains following the vanes, the data presented in the figures could be shifted slightly from what exists at the vane exits.

Examination of the figures reveals that most of the data follow a six cycle variation, which corresponds to the number of vanes, although most of the cycles are not symmetrical. To enable better visualization of the flow patterns, the vector combination of V_θ/V_∞ and V_R/V_∞ are presented in Figure 10, with the length of the arrow proportional to the magnitude of the vector and the direction indicated by the arrow orientation. This figure shows that the flow exiting the vanes is composed of a small vortex or eddy exiting from each vane channel, superimposed on a positive mean swirl.

The formation of the vortices was expected from the vane geometry and is indicated by the inward, then outward appearance of the flow in Figure 10. The fact that the circumferential component of velocity is always positive indicates that some of the mean swirl from the volute still remains after passing through the vanes.

Similar to the representation of the flow in the cross sectional plane, an isometric view of the flow in the axial direction is presented in Figure 11. For the most part, as shown by the figure, the flow is highly irregular. It is also noticed that two large velocity defects exist at approximately 40° and 280°. The exact cause of these defects and the other flow variations, which cannot be attributed totally to wakes from the vanes, is not apparent due to the complexity of the flow. However, several factors which influence the flow can be suggested.

The variations between vane channels must be caused by variations in the flow entering the vanes, since all the vanes are similar. These variations can then cause variations in the formation of separated regions, which in turn can alter the flow in many ways, including the size of the wake shed by each vane. The formation of the vortices is also affected by the vane inlet flow, as shown by Figure 10, which reveals regions where the radial and circumferential components are very small. Both flow separation and the formation of the vortices can contribute to the variations which are observed across one particular vane channel.

Before concluding this section of the report, averaged parameters for each measuring station will be presented, which will aid in the overall evaluation of the system. Since the primary performance criteria are the losses throughout the system, the total pressure is mass averaged at each measuring station. A mass average is employed since the amount of fluid at a particular energy level is as important as the energy level itself. The following equations were evaluated numerically to obtain the mass averaged pressure data. For the throat

$$C_{pT\ \text{mass averaged}} = \frac{\int_0^1 \frac{V}{V_\infty} C_{pT}\, d\left(\frac{d}{h}\right)}{\int_0^1 \frac{V}{V_\infty}\, d\left(\frac{d}{h}\right)} \qquad (1)$$

for the volute inlet

$$C_{pT\ \text{mass averages}} = \frac{\int_0^1 \frac{V_z}{V_\infty} C_{pT}\, d\left(\frac{x}{H}\right)}{\int_0^1 \frac{V_z}{V_\infty}\, d\left(\frac{x}{H}\right)} \qquad (2)$$

and for the test section

$$C_{pT\ \text{mass averaged}} = \frac{\int_0^{2\pi} \int_{r_h}^{r_T} \frac{V_z}{V_\infty} C_{pT}\, r\, dr\, d\theta}{\int_0^{2\pi} \int_{r_h}^{r_T} \frac{V_z}{V_\infty}\, r\, dr\, d\theta} \qquad (3)$$

The average velocity, the mass averaged total pressure coefficient, and the dimensionless flow rate for each station are presented in Table 1. Where several tests had been conducted, the average results are given. The pressure coefficients, which can be subtracted to obtain loss information for a particular component, will be discussed later. For now, an indication of the accuracy of the measurements can be obtained by comparing the flow rates, since in order to satisfy continuity, they should be equal. Using the data at the throat as a reference, the data measured at the volute inlet yields a 4% difference in the calculated dimensionless flow rate. Only a 3% difference is obtained when calculating the flow rate in the test section. Considering that the measurements at the volute inlet and in the test section do not completely define the flow field, particularly near the walls, this information indicates that the measurement made are quite accurate and are at least within only a few percent of the true value.

Discussion

The performance criteria of concern, as mentioned earlier are the uniformity of the flow in the test section and the pressure or energy losses through the various components of the system. Since large losses in the diffuser would be caused mainly by flow separation, identification of any separated zones was also desirable.

It was previously noted, that the results for the volute inlet did not reveal any regions of separated flow. It was also observed that the velocity and total pressure gradients decreased through the diffuser. Since the likelihood of flow separation was lessened by the decreasing of the velocity and pressure gradients, the explanation for this phenomena, which suggest a strong interaction between the volute and the diffuser, was investigated by predicting the velocity and

pressure profiles using several methods.

To help show what effect the volute may have on the upstream flow, free vortex distributions of the z component of velocity and the pressures were computed and are plotted in Figures 8 and 9. A free vortex was used, since the combination of a vortex and a sink can be used to predict the ideal behavior of the flow in a volute. At the inlet to the volute, V_z / V_∞ corresponds to the circumferential component of the vortex sink combination, and V_z/V_∞ depends only on the vortex strength and the distance from the center.

A vortex distribution of the total pressure can also be assumed and will be constant, since a free vortex is an irrotational flow. In this case, the average total pressure upstream was employed. With the total pressure and z component of velocity known, neglecting the x component allowed the static pressure to be calculated also.

Two other methods were used to predict the velocity and pressure profiles at the diffuser exit. These methods predicted the exit conditions from the known inlet conditions, making assumptions similar to those that are made if the inlet flow is uniform. The assumption common to both methods is that the total pressure distribution is unchanged by the diffusion process. This assumption is justifiable under uniform inlet conditions since the total pressure will be changed only by losses. This assumption applied to the present situation, however, results in a discrepancy between the measured and predicted profiles. A comparison of the total pressure distributions predicted by the latter methods with the vortex distribution, suggests that the combination of the two, or the interaction between the volute and the diffuser may cause the experimentally observed profile.

To further investigate the possibility of an interaction, the velocity profile at the diffuser exit can also be predicted from the inlet conditions. This, however, requires an additional assumption. One method is to assume that the static pressure change at every location is identical. The magnitude of this change can be calculated from the difference in the average velocities between the two sections. When the velocity and static pressure are calculated in this manner, the profiles as presented in Figures 8 and 9 result.

The velocity profile predicted using the previous method shows that a steepening of the profile occurs through the diffuser. The calculations performed in obtaining this curve also revealed that the velocity near the top of the diffuser does not possess enough kinetic energy to obtain the required static pressure rise. This fact indicates that if a constant static pressure rise was achieved through the assumed mode of diffusion, flow separation would result.

Once again a combination of the vortex distribution with those just presented could result in the experimentally observed profiles. In particular, a combination of the static pressure gradient in the vortex, with the static pressure field which is obtained assuming ΔP_s = constant, would result in a pressure profile similar to the experimental data. The resulting static pressure gradient could in turn induce the vertical component of velocity which will decrease the velocity and total pressure gradients, as are also indicated by the experimental data.

A third method of predicting the diffuser exit profile was also used. This method rather than assuming a constant change in P_s, assumes each stream tube undergoes the same change in flow area, or in other words, the flow is diffused symmetrically. Results obtained by predicting V_z/V_∞ and the static pressure by this method are also presented in Figures 8 and 9. Surprisingly, the velocity profile is predicted very closely. However, large deviations exist between the predicted and measured pressure profiles. Since the steepness of the total pressure profile can be changed only by flow redistribution, despite the fact that the velocity is accurately predicted, this mode of diffusion is not possible.

All of the previous predictions were made with the intent of demonstrating what effect the volute might have on the flow in the diffuser. Although no definite conclusions can be drawn, the results do indicate an interaction between the volute and diffuser could exist, which would explain the nature of the measured results. Due to the approximate nature of the prediction techiques, experiments should be conducted which would confirm or disprove the interaction.

Continuing now to the other areas of concern, we will consider the uniformity of the flow in the test section and the losses through each component. Little more can be said about the quality of flow leaving the vanes, since the results presented indicate that the flow is highly irregular. At some locations, the vleocity variation is as high at 75% of the mean flow. This large amount of variation could cause severe problems in the pump rotor.

The losses through the diffuser and volute were also larger than hoped. Although, considering the non-uniform nature of the flow at the inlet, we consider the diffuser performance to be quite good. The data obtained for the diffuser can be compared with data in the literature, if the performance is expressed in the conventional pressure recovery coefficient (C_{pr}) and the pressure recovery efficiency (η_p). These parameters are defined by the following equations:

$$C_{pr} = \frac{P_{s_2} - P_{s_1}}{\frac{1}{2}\rho V_1^2} \tag{4}$$

$$\eta_p = \frac{C_{pr}}{[1 - (\frac{A_1}{A_2})^2]} = \frac{\text{actual pressure recovery}}{\text{ideal pressure recovery}} \tag{5}$$

where the subscripts 1 and 2 refer to the inlet and exit of the diffuser respectively.

C_{pr} can be related to the total pressure loss, through the use of the energy equation. After non-dimensionalizing the equation, and replacing the velocity ratio by $\frac{A_1}{A_2}$, we obtain the following expression for C_{pr}:

$$C_{pr} = 1 - (\frac{A_1}{A_2})^2 - \Delta C_{pT_{1-2}} (\frac{V_\infty}{V_1})^2 \qquad (6)$$

Comparisons of C_{pr} and η_p for the diffuser tested, and the predicted data obtained using reference [1] are presented in Table 2. Included in this table are data for the diffuser which would be required by a conventional inlet. Before discussing these values, however, the type of data available in reference [1] should be discussed, since the unusual shape of the present diffuser required some approximations to be made in order to predict its performance.

Data for diffusers with a variety of cross-sectional shapes, circular, square, and rectangular are given in reference [1]. The diffuser geometry most similar to the present diffuser, for which data are available, has a rectangular cross section where two of the walls diverge symmetrically and the other two walls remain parallel. Since the vertical sides of the present diffuser and the diffuser required by a conventional inlet converge, some approximate means of accounting for this effect must be employed.

The design parameters effecting a diffusers performance are the area ratio (A_2/A_1), and the wall divergence angle or the ratio of the diffuser length to the height of the inlet duct. Assuming a constant diffuser width equal to the average width of the real diffuser, the height of diffuser at the inlet and exit can be calculated, which will yield the same areas. Using the previously calculated duct heights, we calculate an equivalent wall divergence angle, which will account for the convergence of the two walls.

The equivalent divergence angle calculated in the previous manner and the real divergence angle, for the current diffuser, both fall below the minimum value for which the angle causes a significant effect on the pressure recovery. Therefore, the predicted results should be accurate if it were not for the effect caused by the non-uniform inlet flow. However, for the diffuser required by a conventional inlet, the equivalent and real divergence angle differ greatly, and the real divergence angle lies in a region on the perfromance curve where significant losses due to separation will occur. Therefore, even though the pressure gradient may not be excessive, the large divergence angle of the diverging walls could cause separation losses not indicated in the predicted results.

Refering now to Table 2, it is seen that the efficiency of the diffuser tested has approximately a 14% lower efficiency than the performance predicted using the data of Reference [1]. This reduction in performance is probably primary due to the shearing nature of the flow caused by the velocity gradients. This source of loss is unavoidable, and since flow separation was avoided, significant improvements in the diffuser performance appear unlikely. One other additional source of

losses, which may be causing part of the indicated performance reduction, could be the energy dissipated by the additional turbulence caused by the inlet wires. The determination of the magnitudes of these losses would require further experimentation.

Also included in Table 2, is the predicted performance of the diffuser required by a conventional inlet. The diffusion necessary for a conventional inlet is greater than the overall diffusion required, since the flow must be accelerated at the impeller inlet to improve the flow characteristics. The predicted values were included in the table to demonstrate the additional losses which would result if a conventional inlet was used.

The predicted performance for the conventional inlet diffuser should not be compared with the experimental data for the present diffuser, since the prediction does not include the losses due to the shear flow. However, comparison with the prediction for the diffuser which was tested, does indicate the reduction in performance which could be expected. This reduction is also probably underestimated since the large divergence angle of two of the walls and the non-uniform inlet velocity would most likely result in flow separation.

The losses through the volute and vanes should also be compared with data available in the literature to evaluate its performance. Since the purpose of the volute is to turn the flow 90°, the losses can be compared to the losses in conventional pipe bends. Losses for pipe bends are usually expressed in the form of a loss coefficient (K_L), which is defined by the following equation:

$$h_L = K_L \frac{V^2}{2g} \qquad (7)$$

where h_L = head loss
K_L = head loss coefficient
V = average velocity
g = acceleration of gravity

The value of K_L for the volute was determined to be 1.44. The losses represented by this large value of K_L are even higher than those which occur in a sharp 90° miter pipe bend. For a miter bend, K_L is approximately 1.1 [2]. Most of the pressure losses in the volute are probably caused by flow separation off the back of the vanes, and the energy dissipated in the vortices which are formed. To make matters worse, some of the total energy measured in the test section, is not useful, since most of the energy in the measured vortices will be dissipated.

Summary and Conclusions

Results from the test program have been presented and discussed. The data indicate no flow separation occured in the diffuser, but the losses were slightly higher than expected. The possibility of an interaction between the diffuser and the flow in the volute was also investigated by approximate techniques. These techniques provide sufficient evidence of an interaction to justify additional experimental studies. If future studies prove a strong interaction does exist, which prevents flow separation, motivation for the improvement and use of a vaned

volute will be increased. Even if flow separation is not prevented by the volute, the additional diffusion and large wall divergence angles of a conventional inlet diffuser, would probably result in separation. This possibility also supplies increased motivation for the use of a volute.

The performance of the volute and vane system was not encouraging. The flow leaving the volute was shown to be very non-uniform and the pressure losses were great. The primary cause of the non-uniformity and the losses is suspected to be the formation of the observed vortices in each vane channel. Therefore, a new type of vane system, which eliminates the vortex formation, could possibly cure both problems, high losses and the non-uniform flow.

Recommendations for Improvements and Future Studies

1. The extent of the losses through the diffuser, which are caused by the shear flow and the turbulence generated by the inlet wires, can be investigated by testing the diffuser under uniform inlet flow conditions. Total pressure measurements at several locations upstream of the throat could also be made with the wires present, to determine the rate at which the energy of the flow is dissipated by the wire induced turbulence. Since the velocity profile will retain a constant shape through most of the inlet, changes in the rate of pressure loss will be caused primarily by the decrease in the turbulence level. Data from these measurements could then be extrapolated to approximate the losses in the diffuser caused by the artificially generated turbulence. This data is necessary if a true indication of the diffusers performance is to be obtained.

2. The interaction between the volute and the diffuser should be investigated experimentally to determine if flow separation in the diffuser is prevented by the induced effects of the volute. The amount of interaction can be checked easily by simply replacing the volute by a straight section and then measuring the resulting velocity and pressure profiles at the diffuser exit. This study could be accomplished with minimal changes to the present system.

3. With information gained from the present study a new type of vaned volute should be designed, built, and tested. When considering the possibilities for alternate vane systems, two broad categories are possible, an axial flow or radial flow vane channel. Axial flow type vanes could be located in an axial section just downstream of a plain volute. Preliminary calculations, however, reveal that the resulting circumferential component of velocity would be to great for this type of vane to be practical.

   The only other apparent possibility is to design a radial flow vane channel, which will begin to remove the swirl created by the volute before excessively large components of circumferential velocity are created. The volute and vanes of the present system fall in this category, however, with knowledge from the present study, the design method could be greatly improved.

   The present volute and vanes were designed primarily from a 2-dimensional analysis of the flow in the plane of the volute spiral. Insufficient considerations were given to the flow in the meridional plane, which must still negotiate a sharp 90° turn. It becomes apparent that the meridional flow channel should be given primary

consideration, which essentially means the radius of the curve leading into the axial direction must be increased. The shape of this section could be designed following conventional radial flow pump or turbine practice.

Once the shape of the meridional passage is chosen, a volute can be designed which will evenly distribute the flow to the passage. Radial measurements in the existing volute could be made to help predict the flow distirbution in the new volute.

With the design of the meridional passage and the volute fixed, the vanes can be designed once again employing conventional pump or turbine design. The inlet angle will be known from the predicted flow distribution in the volute, and the exit angle is known, since the flow should be axial. The vanes may be designed with a 2-dimensional profile, if it is necessary to reduce costs. It should be noted that the greater circumferential extent of the new vanes will increase the effective radius of the meridional flow passage, thus the axial length should not be increased significantly.

It had been suggested, that additional vanes be added to the present volute in order to make the exit flow more uniform, and eliminate the remaining amount of mean swirl. Although additional vanes probably would prevent or reduce the size of the vortices which are formed, the losses would probably be increased significantly. Since the losses are already above a tolerable level, little could be gained by making this modification.

4. It would be desirable to have data from a conventional type inlet, which would allow performance comparisons to be made. Comparison of the volute performance with a mitered bend were made in the discussion of the results. This comparison indicated that the present volute can not compete with a conventional inlet. However, if a new volute is designed and built, which demonstrates significant performance improvements, it may be necessary to design, build, and test a conventional inlet in order to choose the right inlet for the pumps in the planning craft. Although data for a conventional inlet may be available from other sources, testing an inlet under the same conditions as the volute will be required for accurate comparisons.

References

1. Norris, R. Hasmer, Florence F. Buckland, Nancy D. Fitzroy, "Fluid Flow Data Book," Schenectady, N.Y., General Electric Co. Corporate Research and Development, 1970.

2. Vennard, J. K., "Elementary Fluid Mechanics," 4th Edition, John Wiley & Sones, Inc., 1961.

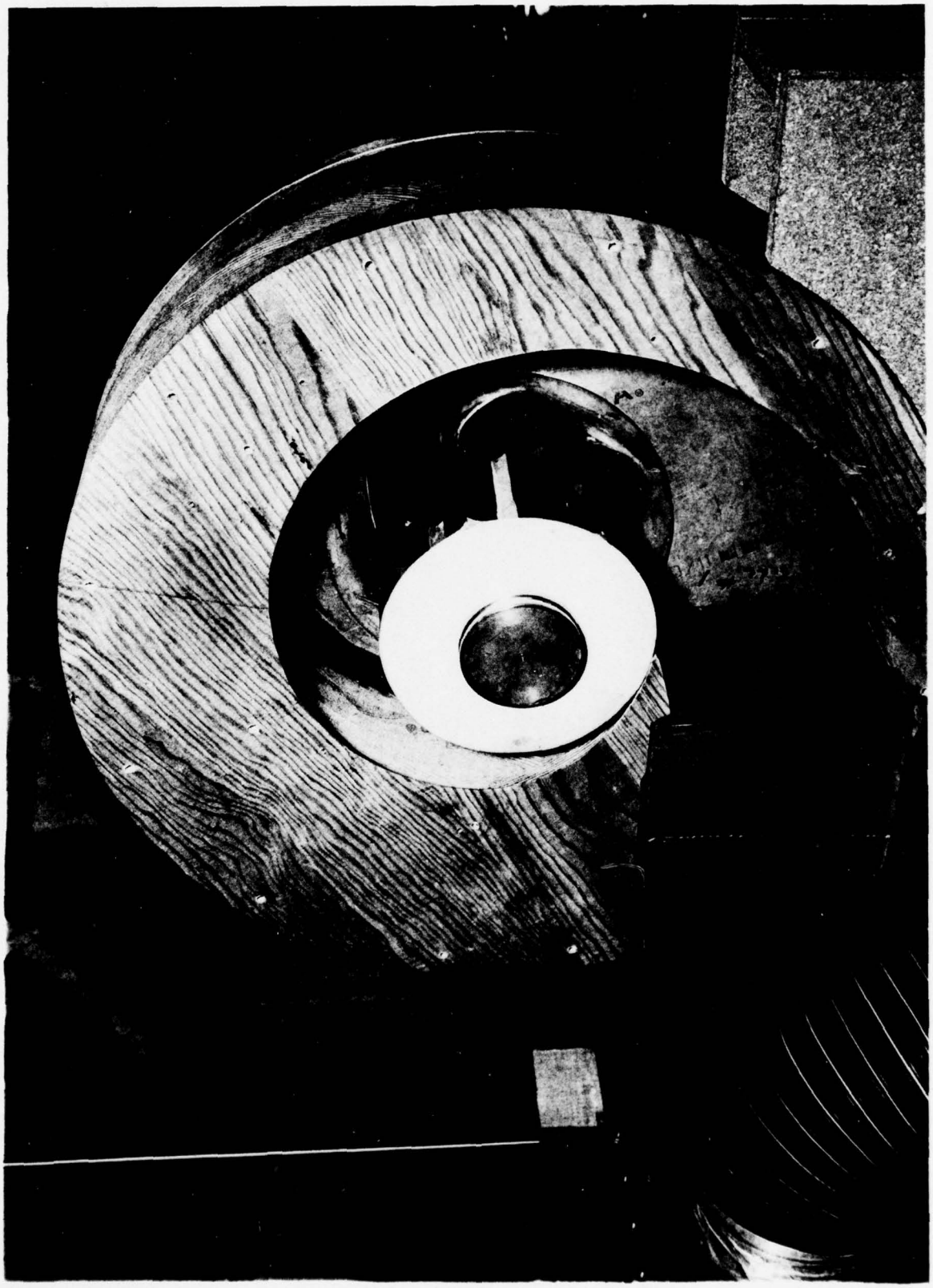

Figure 1 A close-up of the volute and the vanes.

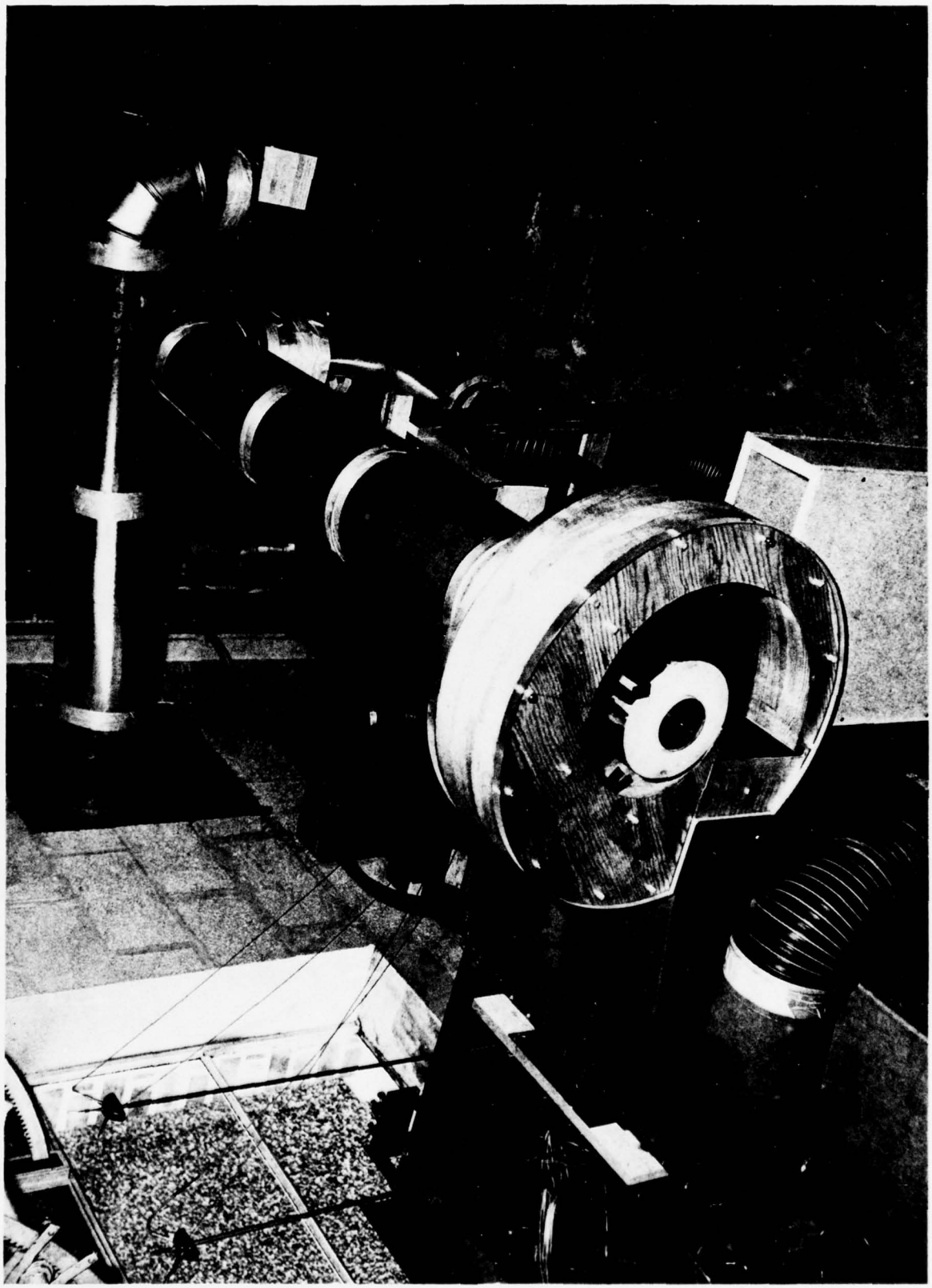

Figure 2 An overall view of the test facility.

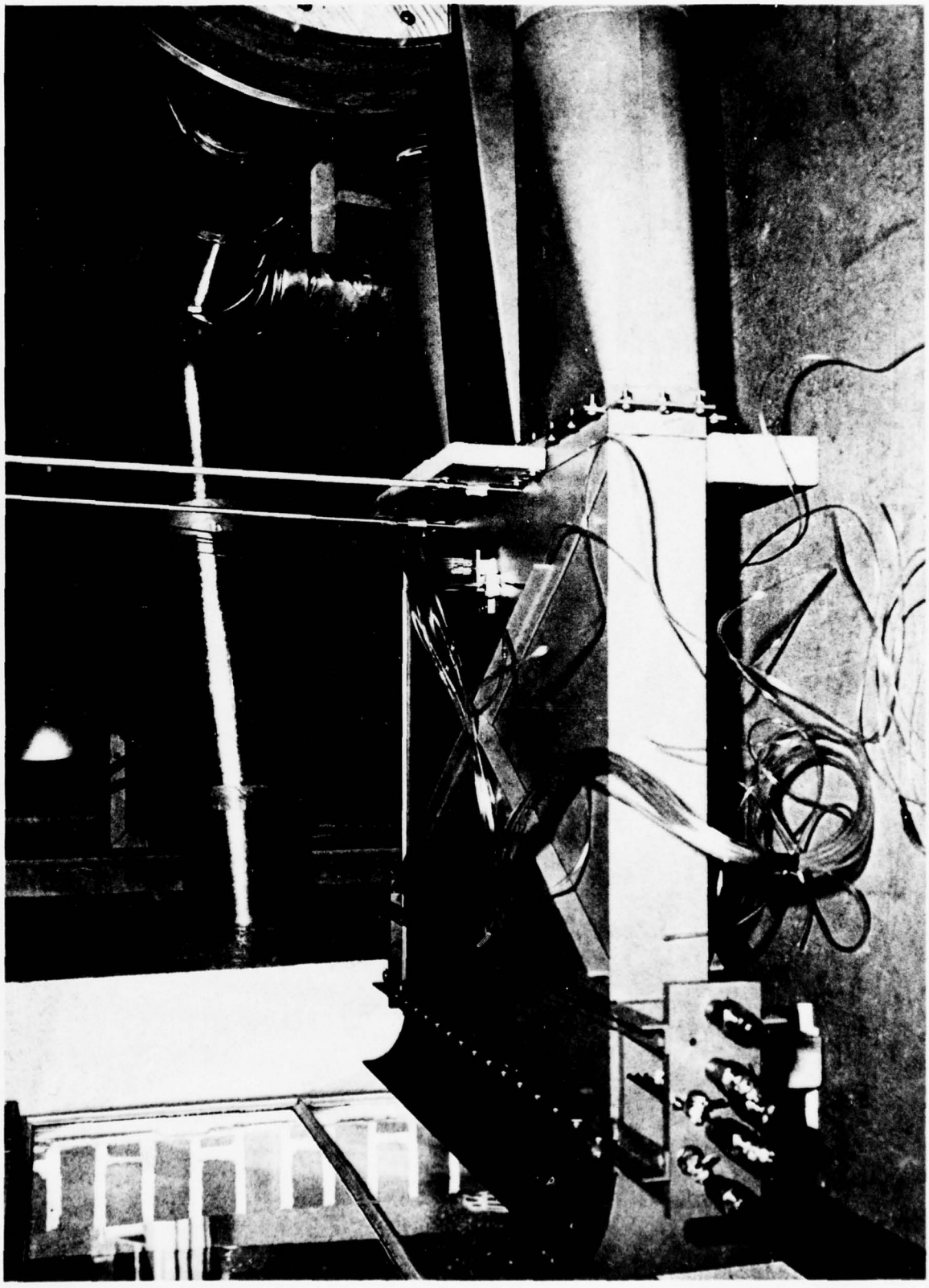

Figure 3 A view of the inlet section of the test facility.

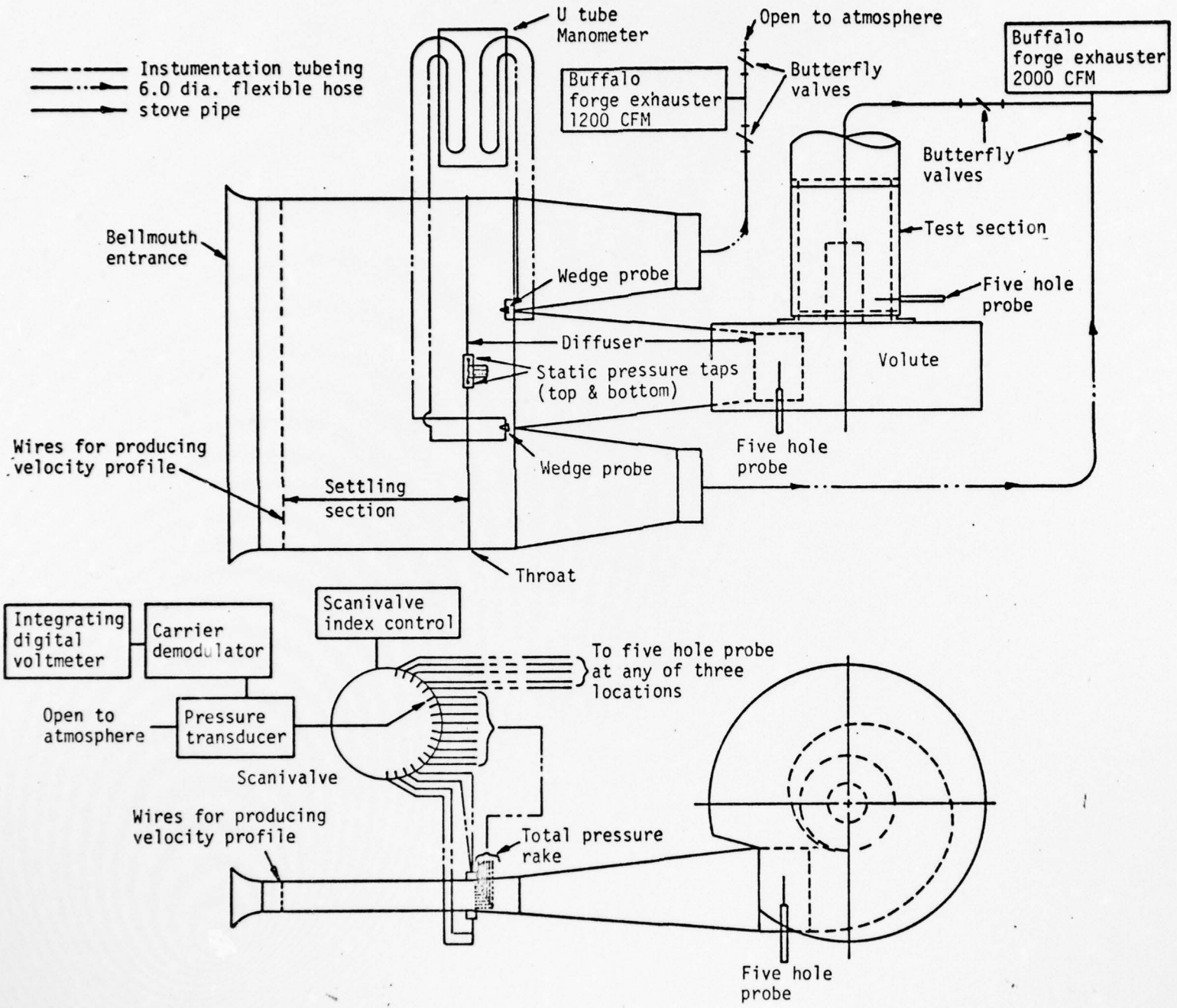

Figure 4 A schematic of the test facility and the instrumentation.

February 8, 1977
AY:tms

February 8, 1977
AY:tms

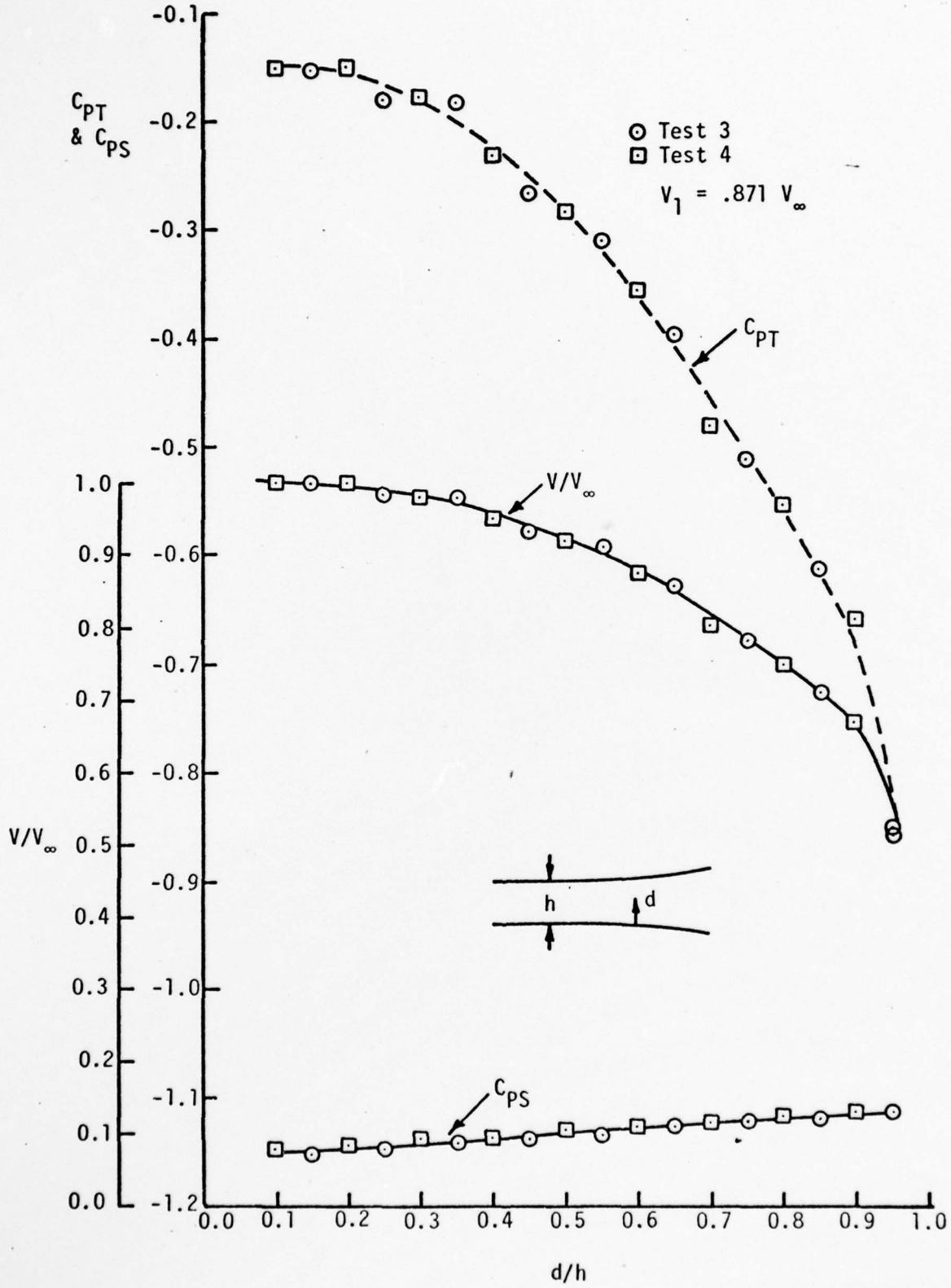

Figure 5 Velocity and pressure profiles measured at the throat.

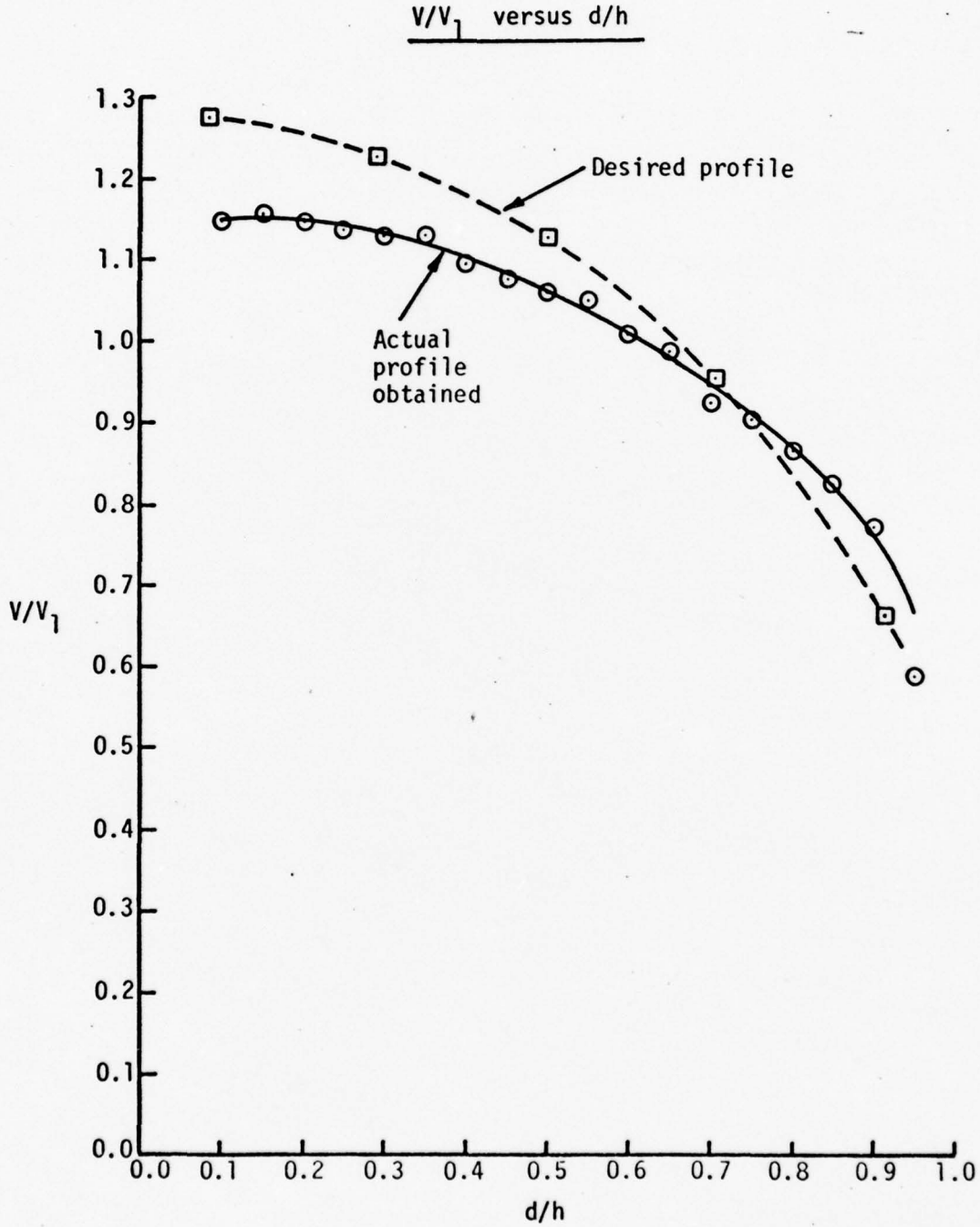

Figure 6 Comparison of the experimental data with the design data at the throat.

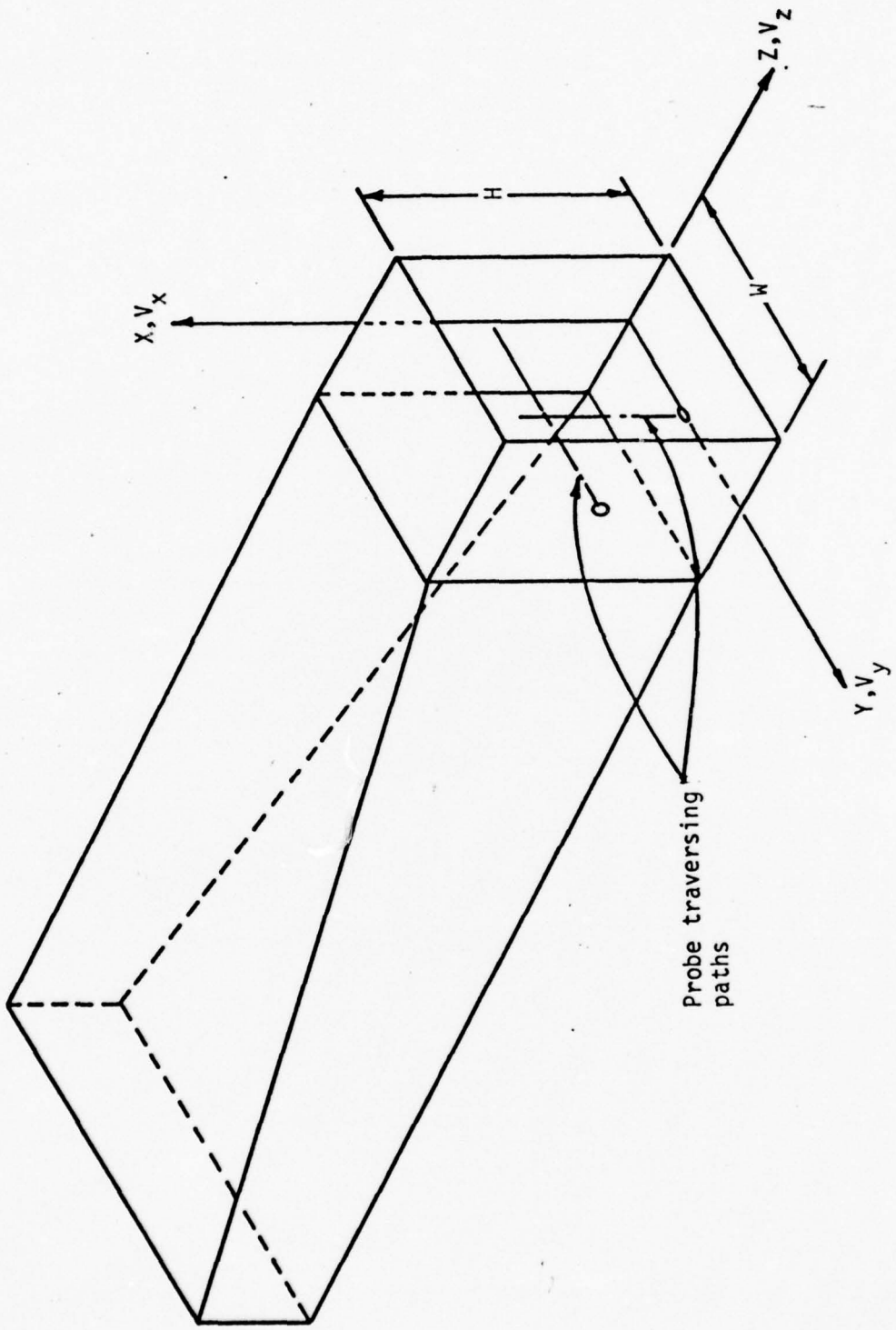

Figure 7 Schematic of the diffuser exit showing the location of the traverses and the coordinate system used in presenting the data.

February 8, 1977
AY:tms

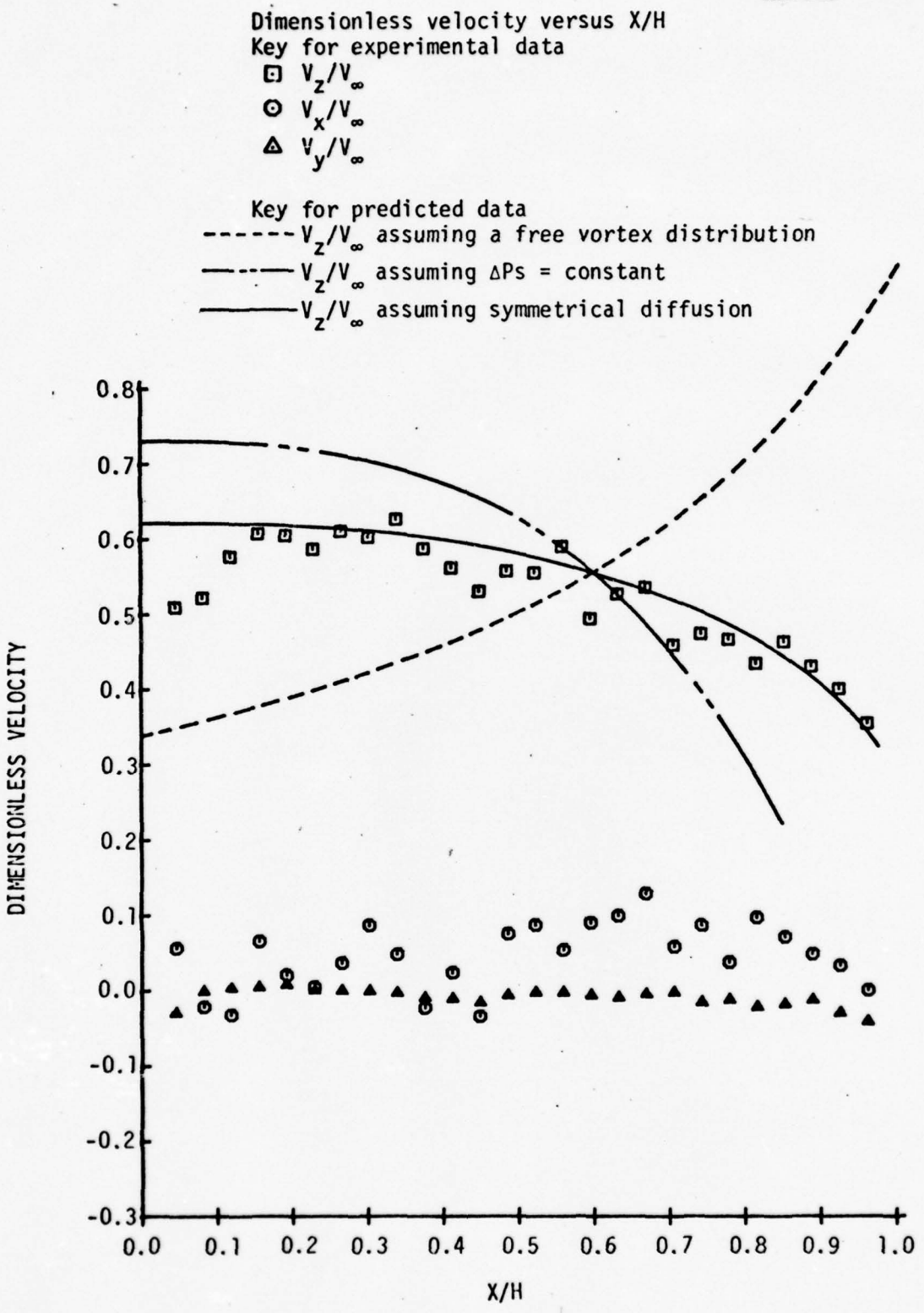

Figure 8 Predicted and measured velocity profiles at the volute inlet.

February 8, 1977
AY:tms

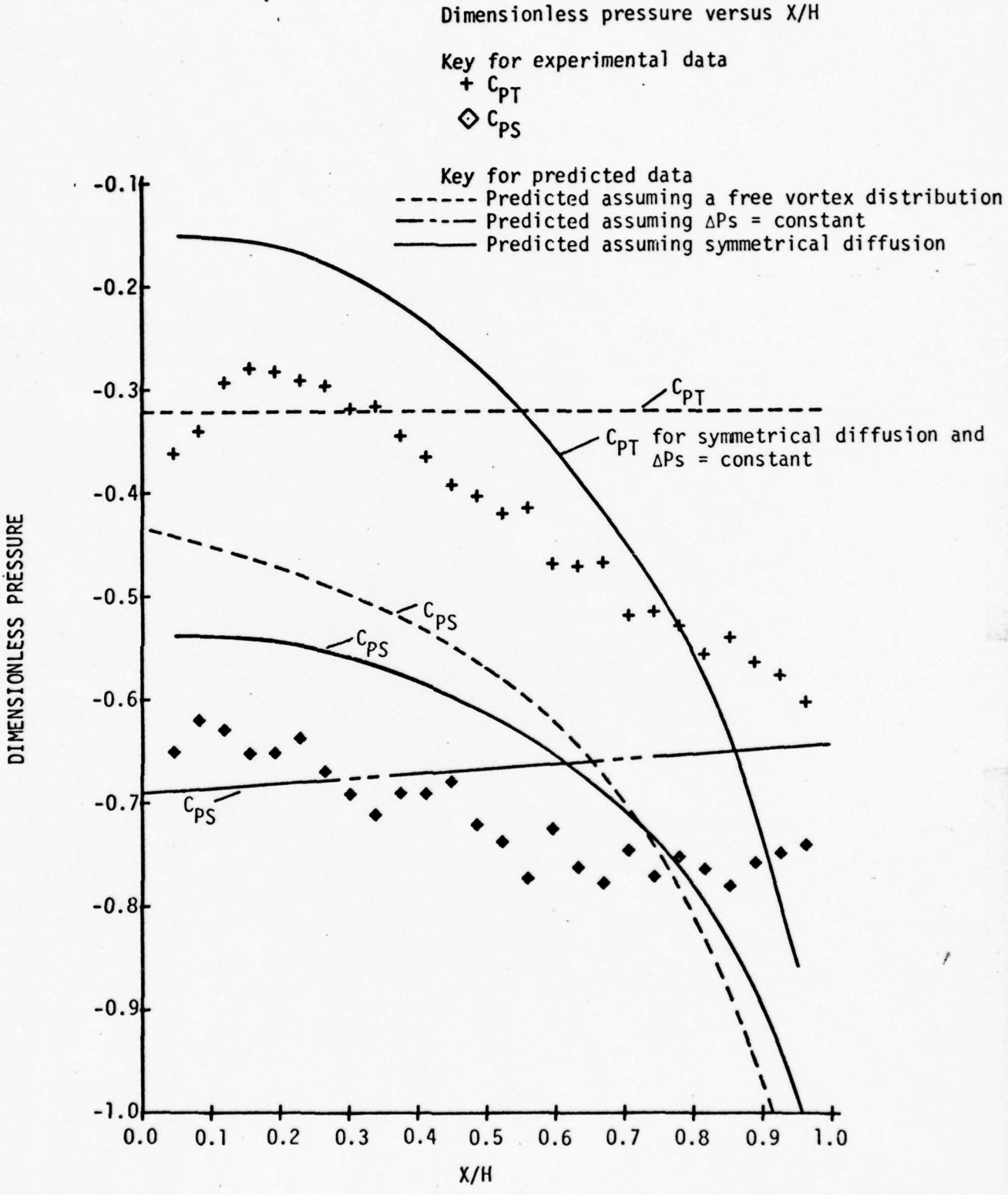

Figure 9 Predicted and measured pressure profiles at the volute inlet.

February 8, 1977
AY:tms

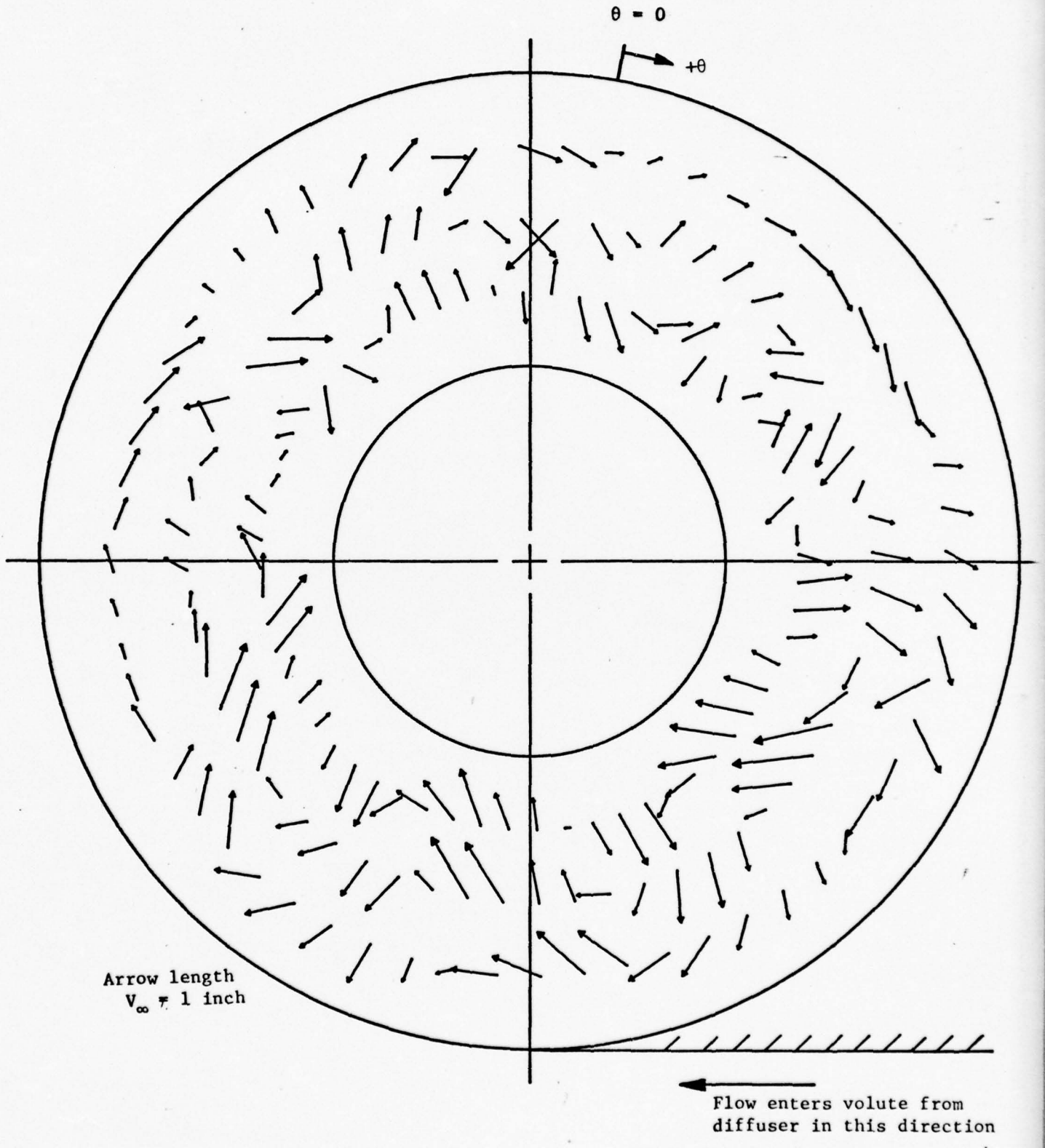

Figure 10 A cross sectional view of the test section, with the dimensionless velocity vectors in this plane represented by arrows.

$$\frac{V}{V_\infty} = \frac{\sqrt{V_\theta^2 + V_r^2}}{V_\infty}$$

February 8, 1977
AY:tms

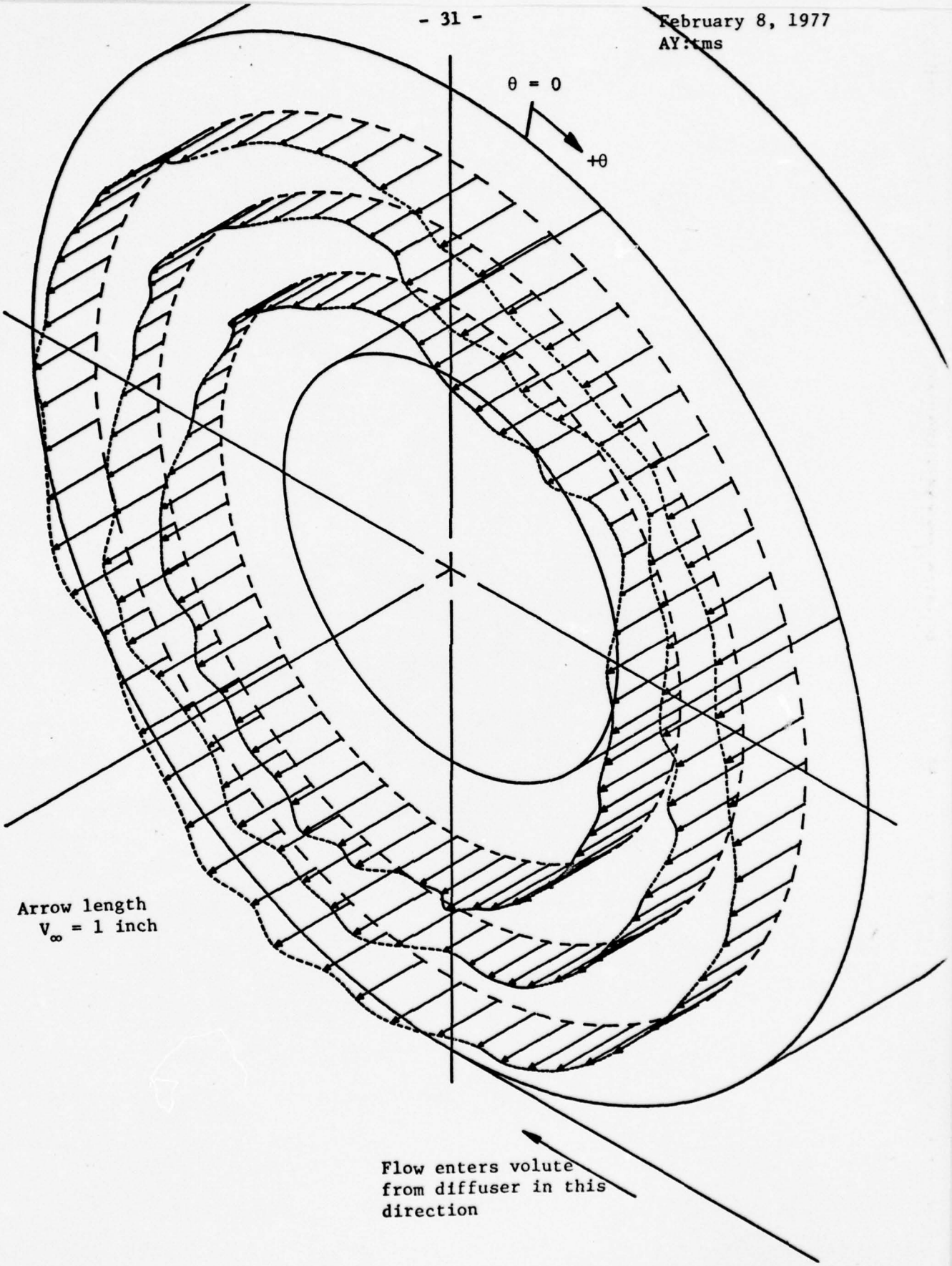

Figure 11 Isometric drawing of the measurement station downstream of the volute, with V_z/V_∞ represented by arrows.

Table 1

Average parameters calculated for each measurement station.

	Throat	Volute Inlet	Test Section
$\frac{V_z}{V_\infty}$ avg.	.8709	.5198	.5670
C_{pT} mass avg.	-.3217	-.4090	-.8704
$\frac{V_{z\ avg.} A}{V_\infty A_1}$	.8709	.8357	.8978

Table 2

Measured and predicted diffuser performance parameters.

	A_2/A_1	C_{pr}	η_p
Present diffuser (experimental)	1.61	.498	.812
Present diffuser (predicted)	1.61	.586	.956
Diffuser for a conventional inlet	2.57	.762	.898

Appendix A

Data taken at the volute inlet

February 8, 1977
AY:tms

DIMENSIONLESS VELOCITY VERSUS X/H
VERTICAL TRAVERSE RUN V-1

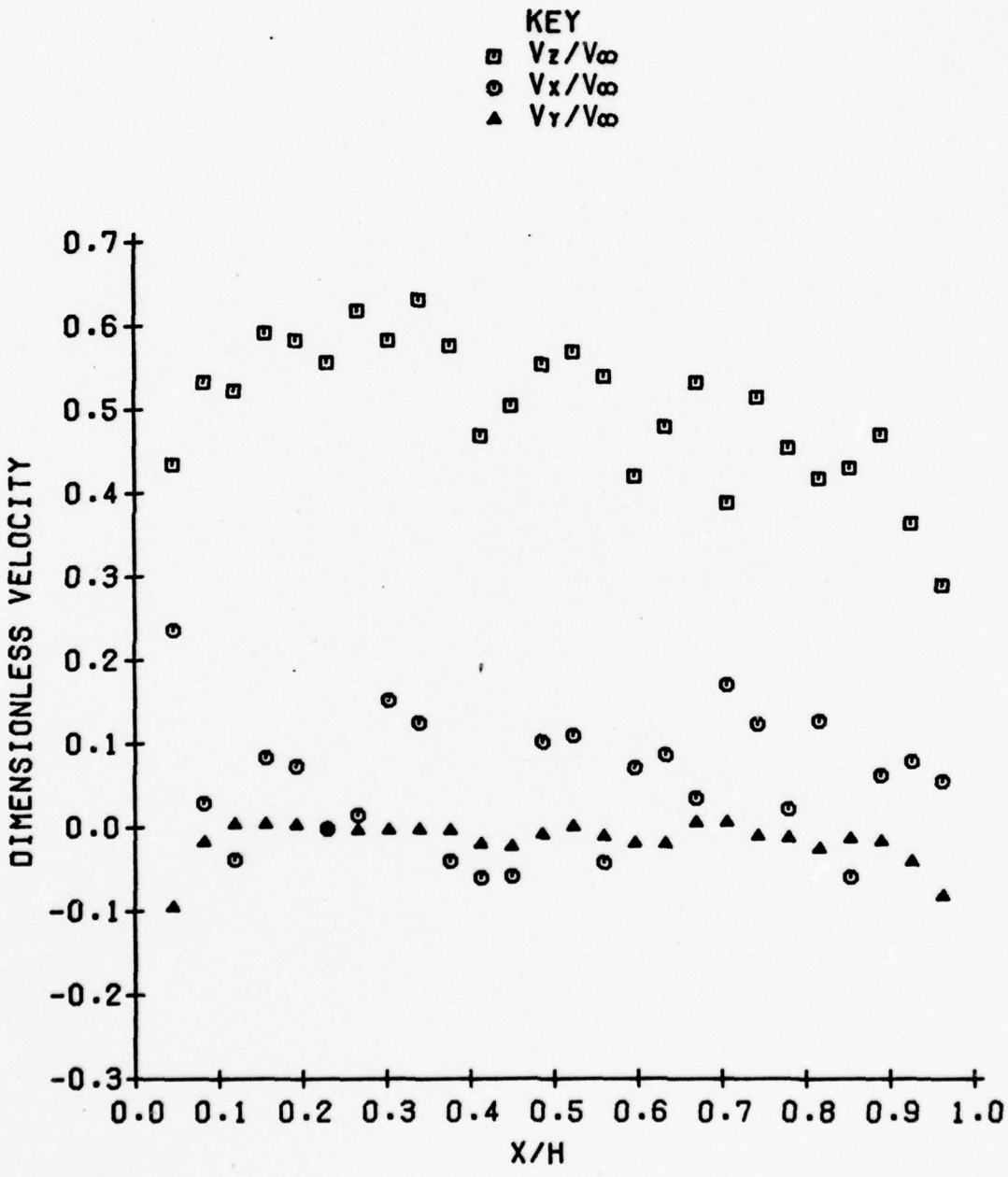

Figure A.1 Data taken at the volute inlet.

February 8, 1977
AY:tms

DIMENSIONLESS VELOCITY VERSUS X/H
VERTICAL TRAVERSE RUN V-2

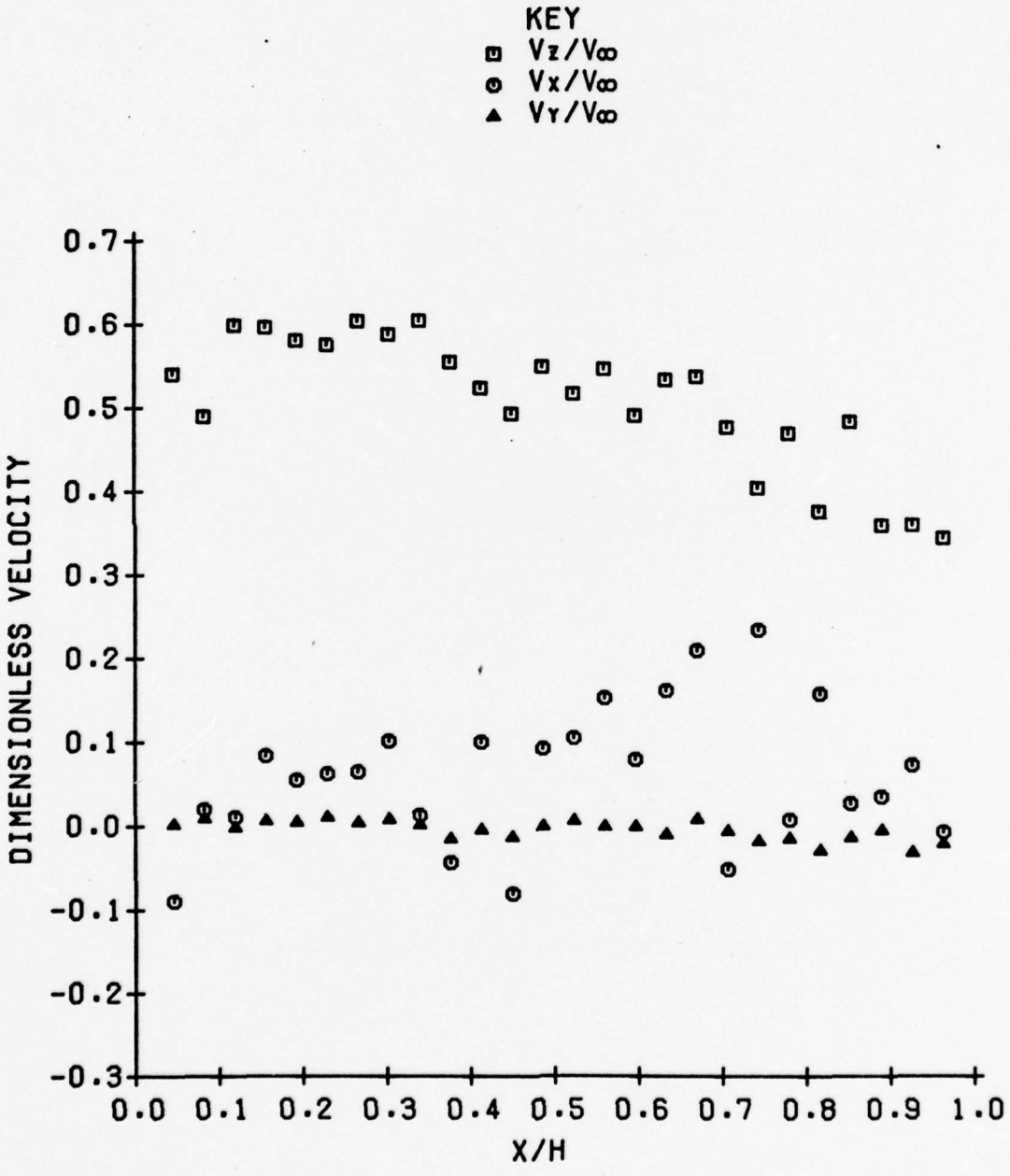

Figure A.2 Data taken at the volute inlet.

February 8, 1977
AY:tms

DIMENSIONLESS VELOCITY VERSUS X/H
VERTICAL TRAVERSE RUN V-3

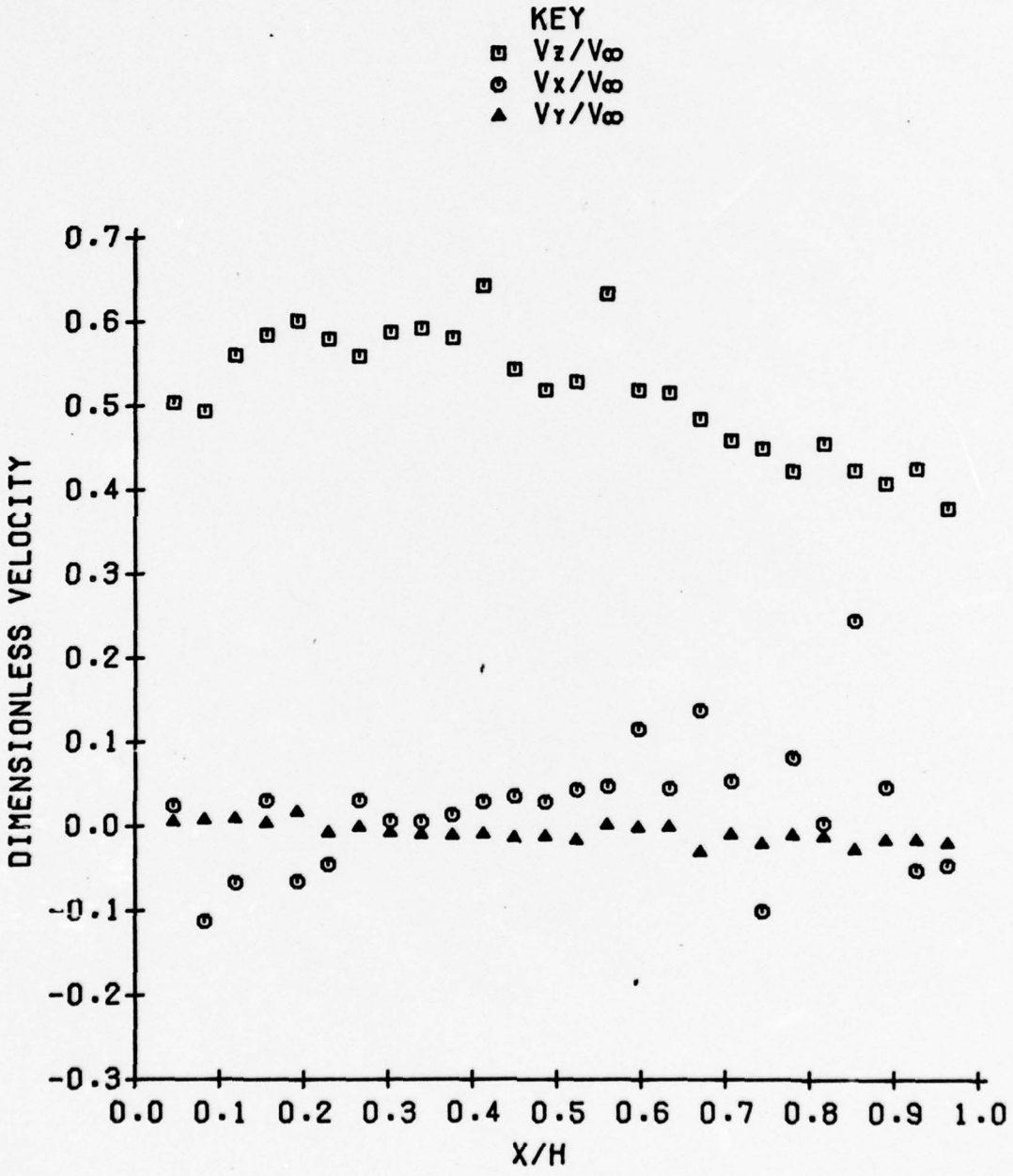

Figure A.3 Data taken at the volute inlet.

February 8, 1977
AY:tms

DIMENSIONLESS PRESSURE VERSUS X/H
VERTICAL TRAVERSE RUN V-1

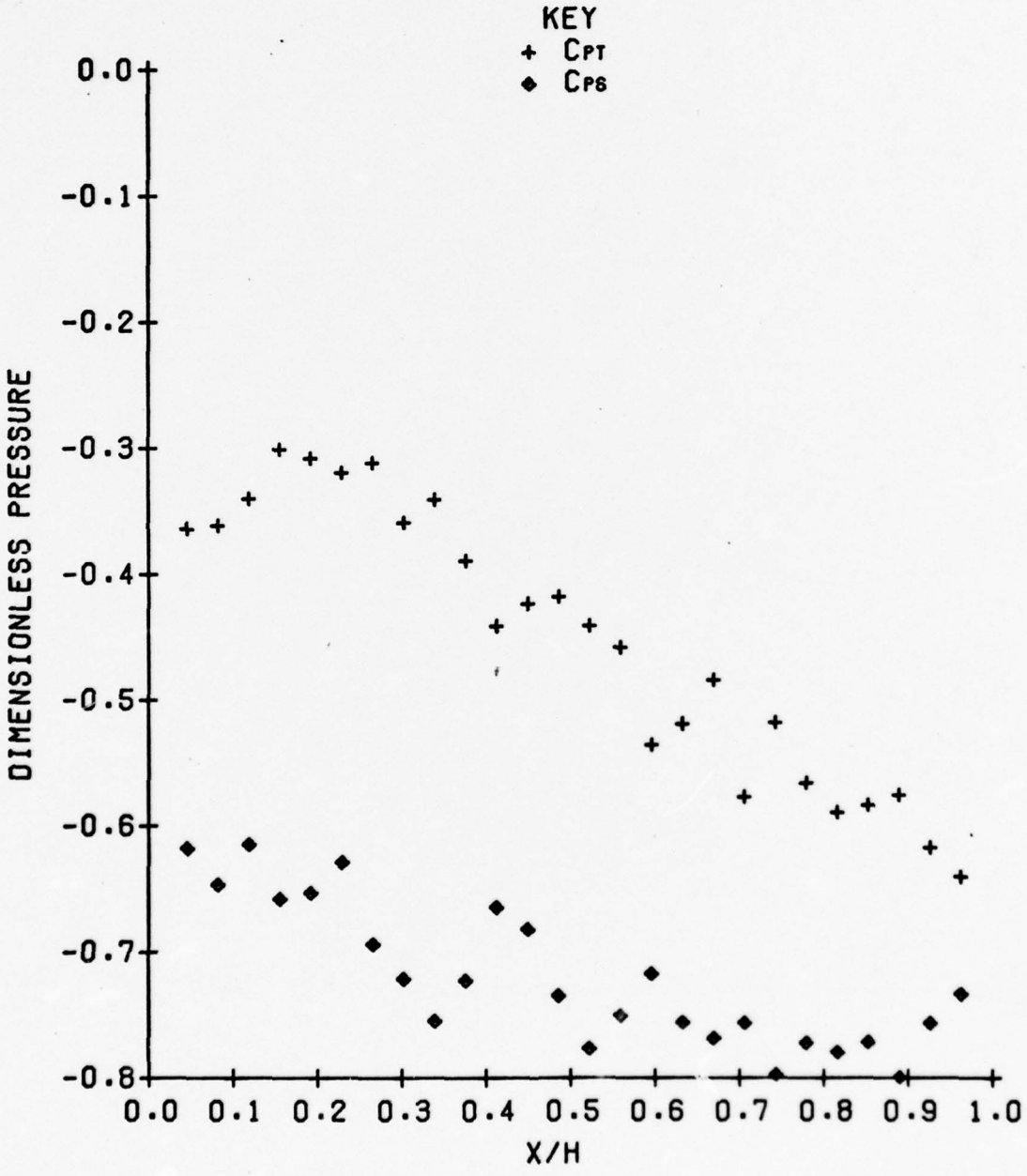

Figure A.4 Data taken at the volute inlet.

February 8, 1977
AY:tms

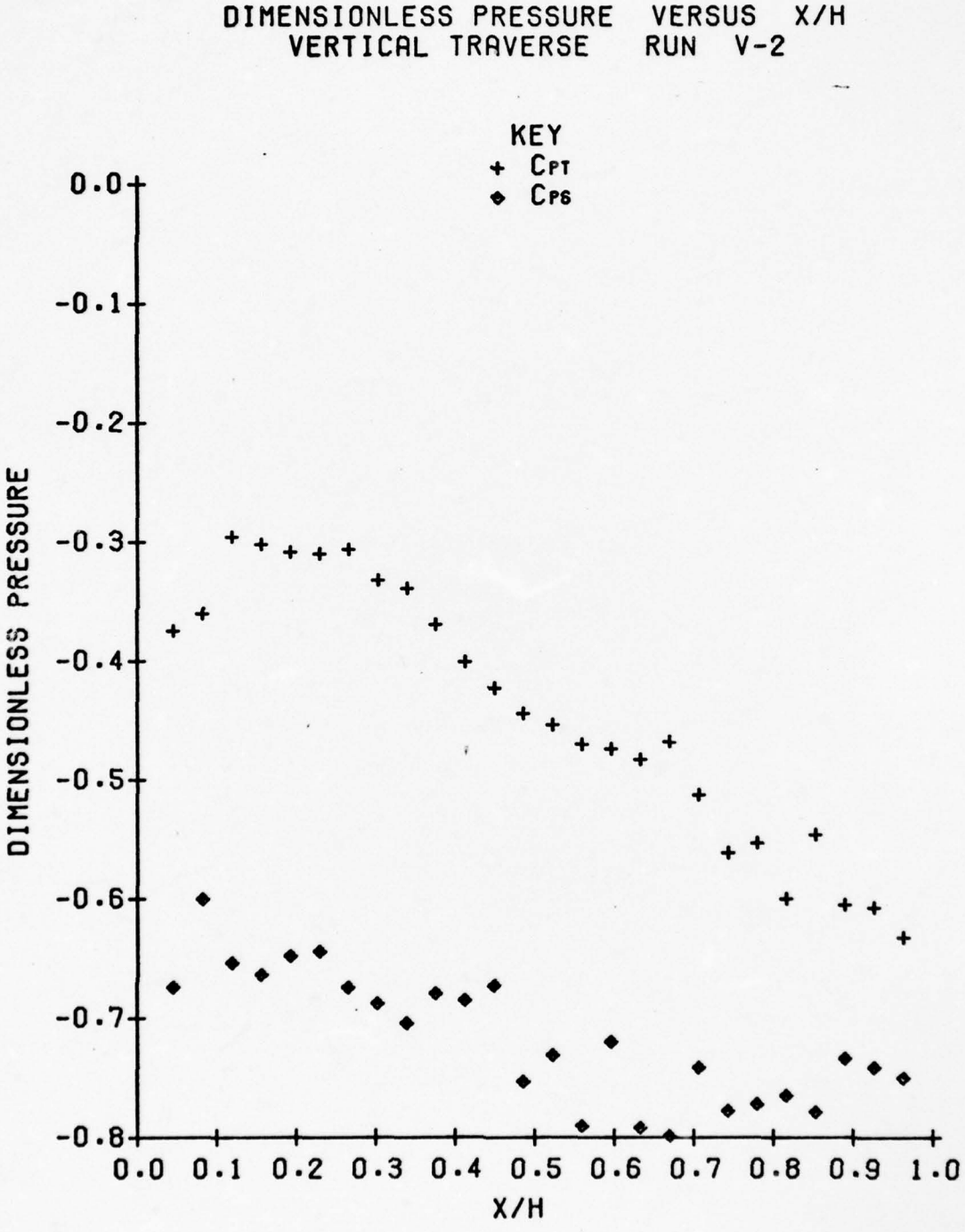

Figure A.5 Data taken at the volute inlet.

February 8, 1977
AY:tms

DIMENSIONLESS PRESSURE VERSUS X/H
VERTICAL TRAVERSE RUN V-3

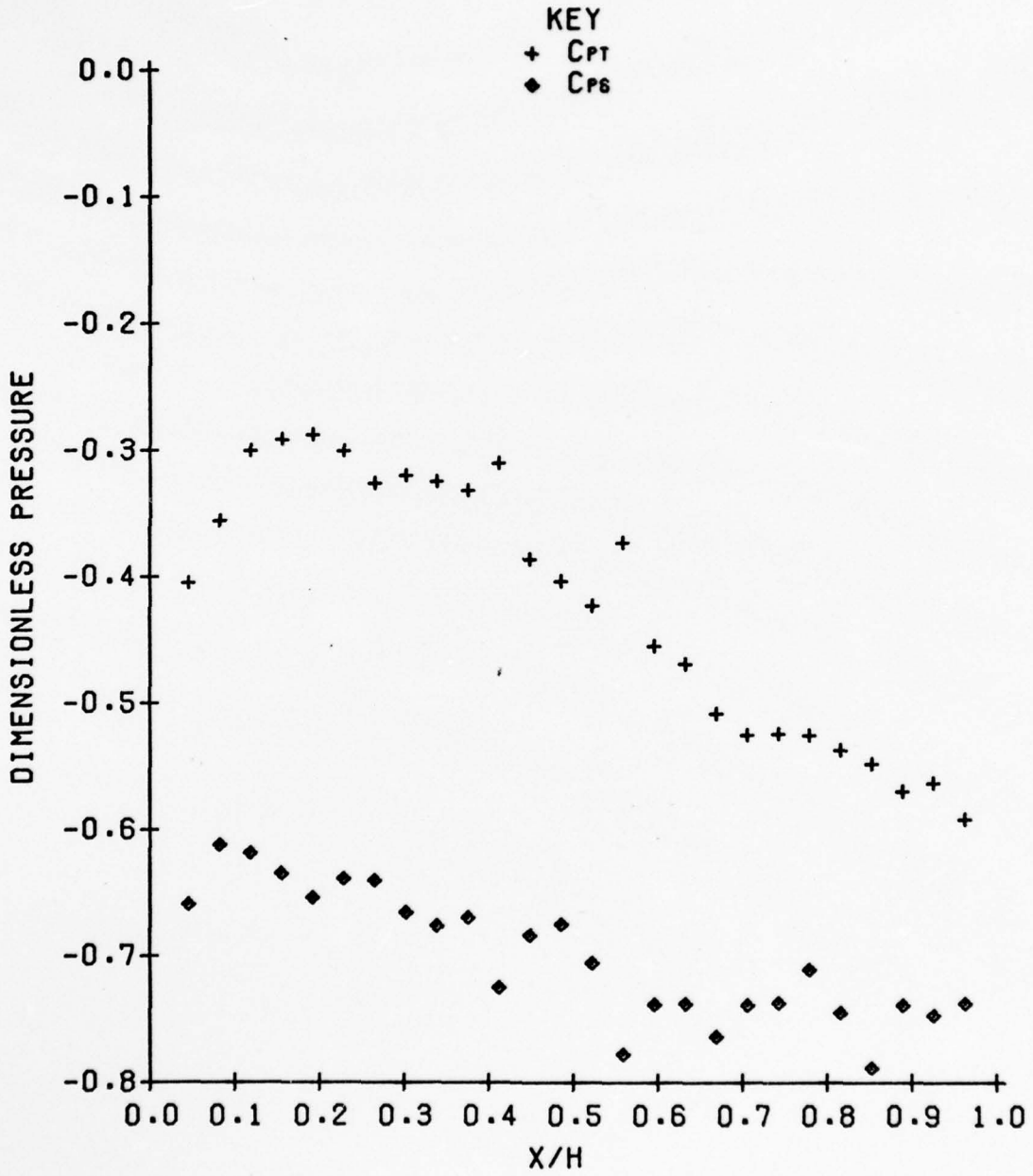

Figure A.6 Data taken at the volute inlet.

February 8, 1977
AY:tms

DIMENSIONLESS VELOCITY VERSUS Y/W
HORIZONTAL TRAVERSE RUN H-1

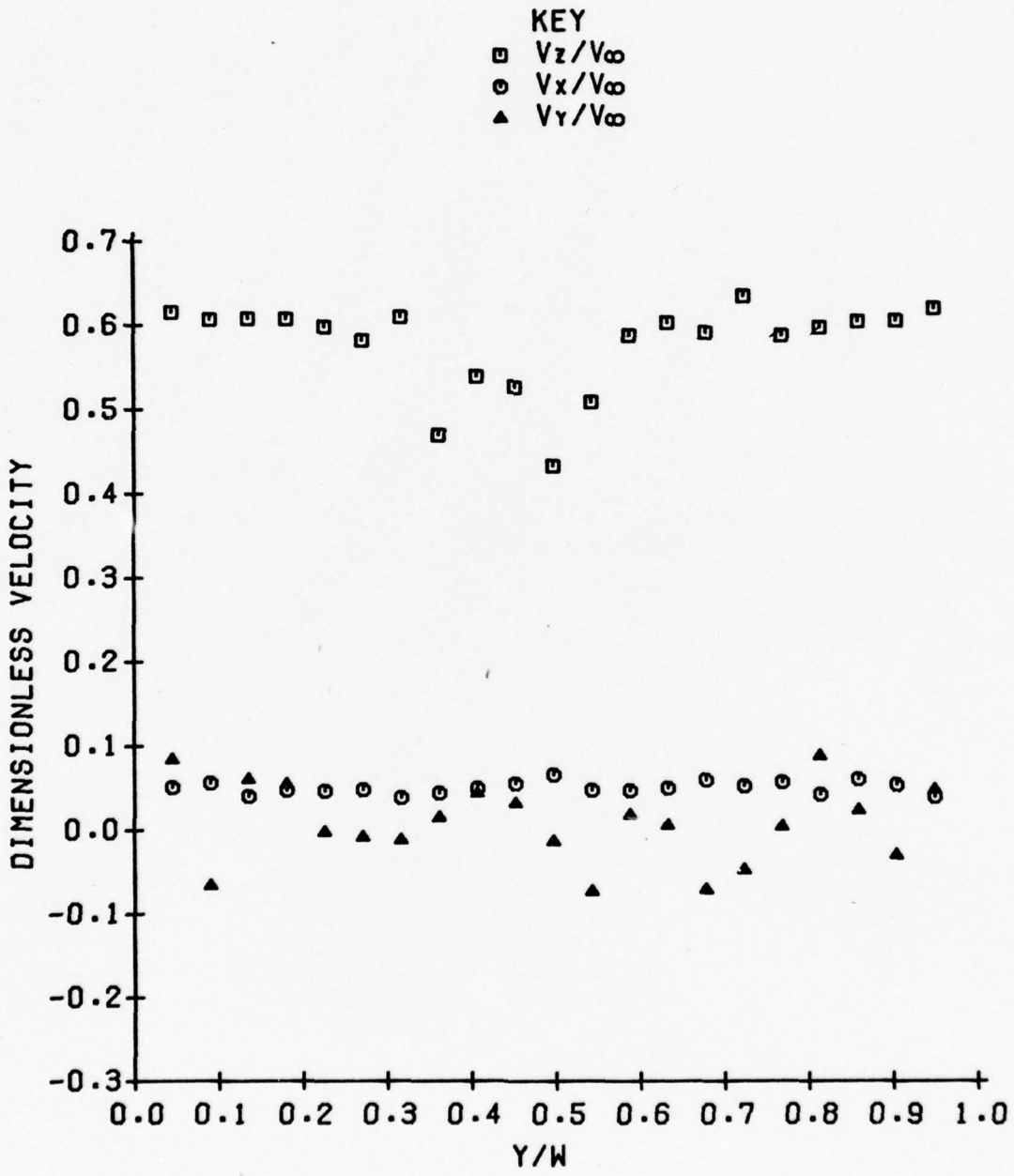

Figure A.7 Data taken at the volute inlet.

February 8, 1977
AY:tms

DIMENSIONLESS VELOCITY VERSUS Y/W
HORIZONTAL TRAVERSE RUN H-2

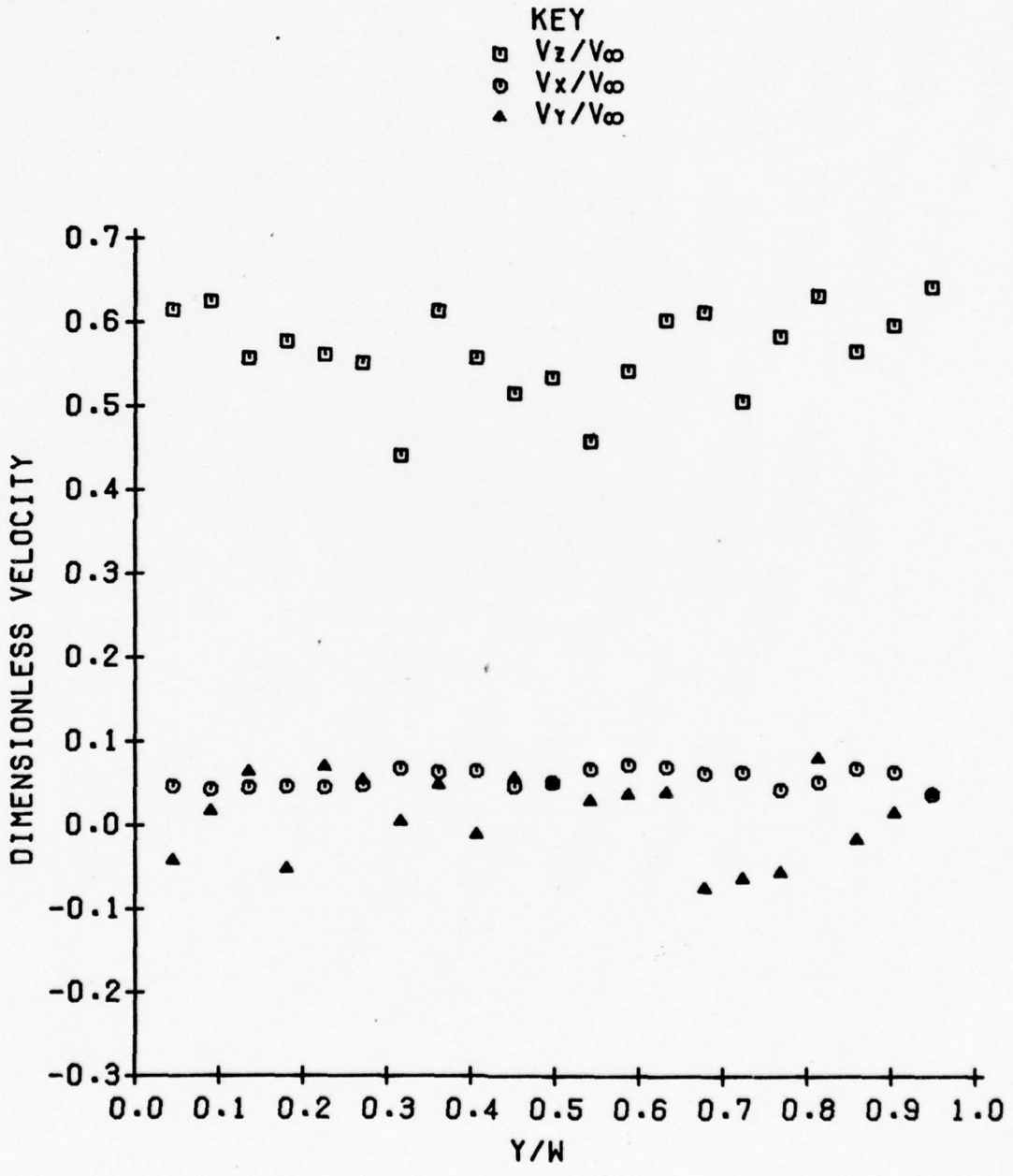

Figure A.8 Data taken at the volute inlet.

February 8, 1977
AY:tms

DIMENSIONLESS VELOCITY VERSUS Y/W
HORIZONTAL TRAVERSE RUN H-3

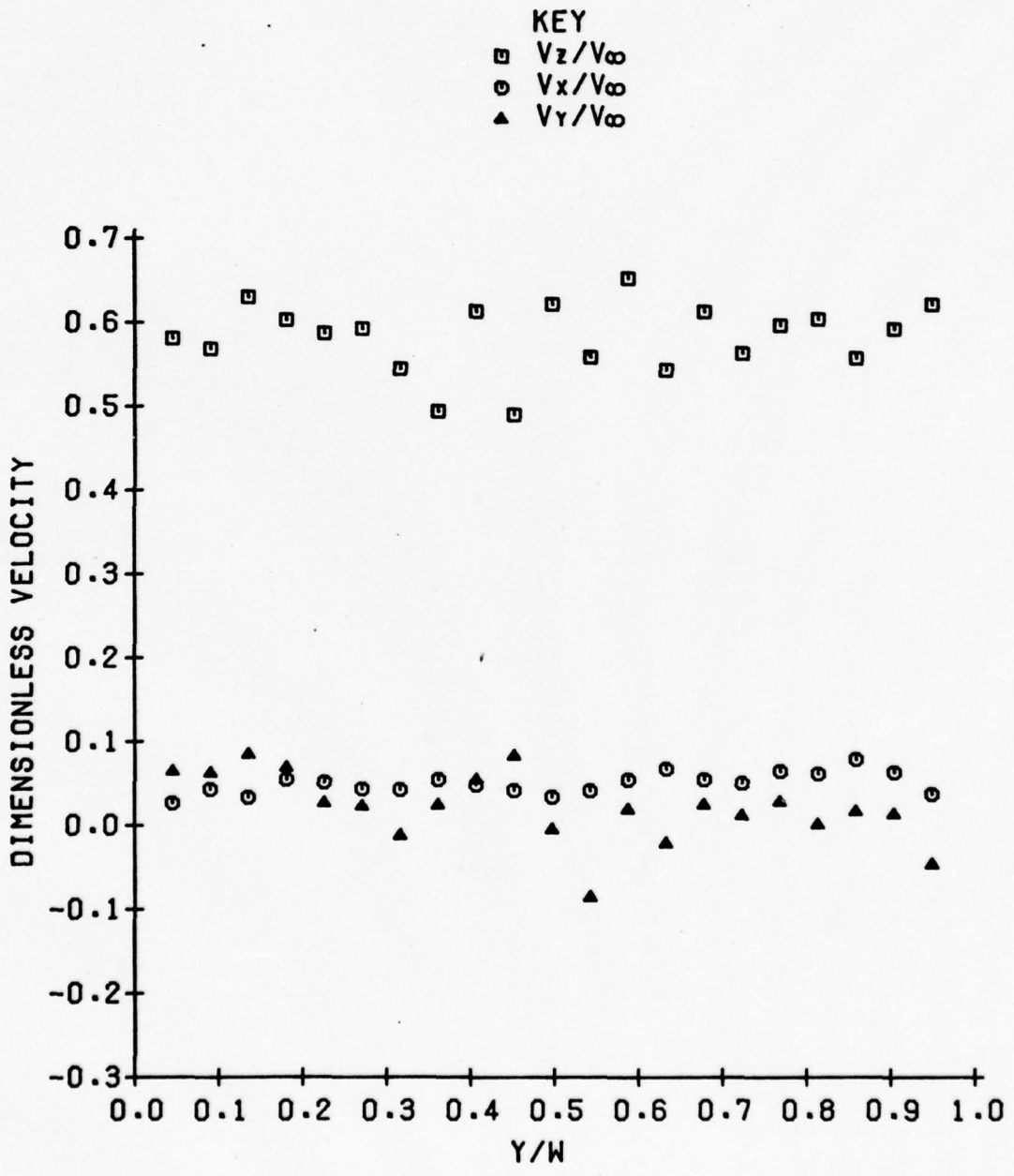

Figure A.9 Data taken at the volute inlet.

February 8, 1977
AY:tms

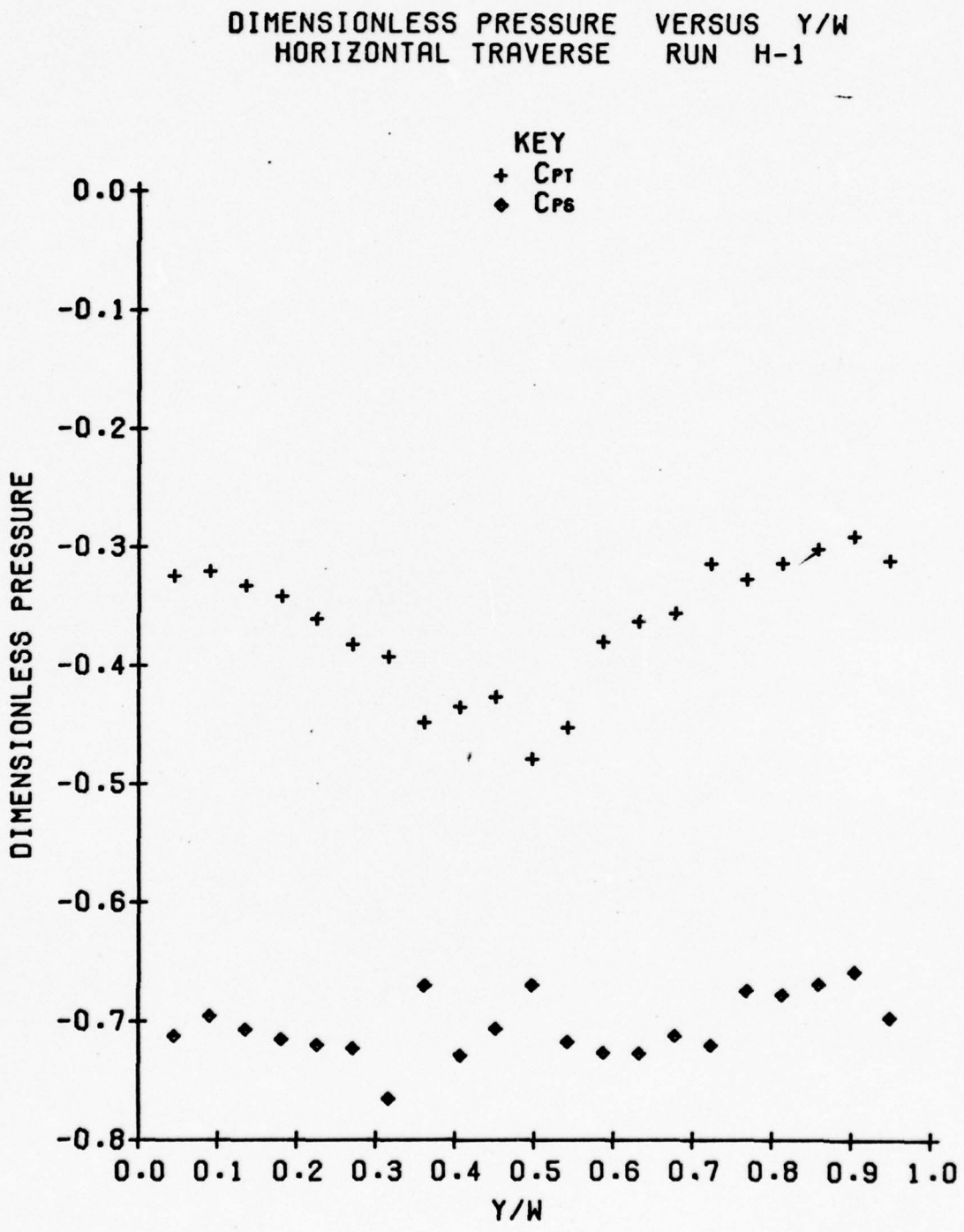

Figure A.10 Data taken at the volute inlet.

February 8, 1977
AY:tms

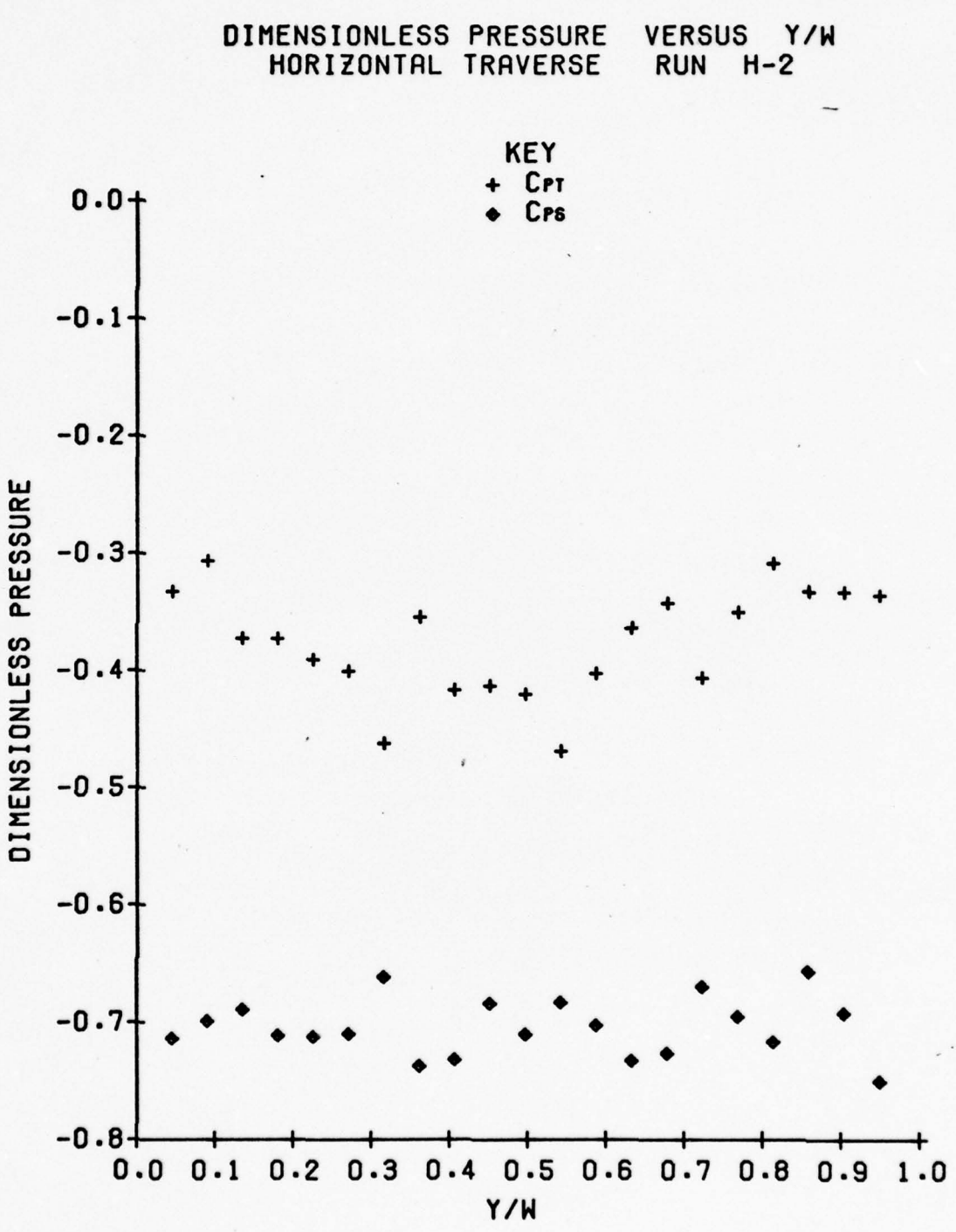

Figure A.11 Data taken at the volute inlet.

February 8, 1977
AY:tms

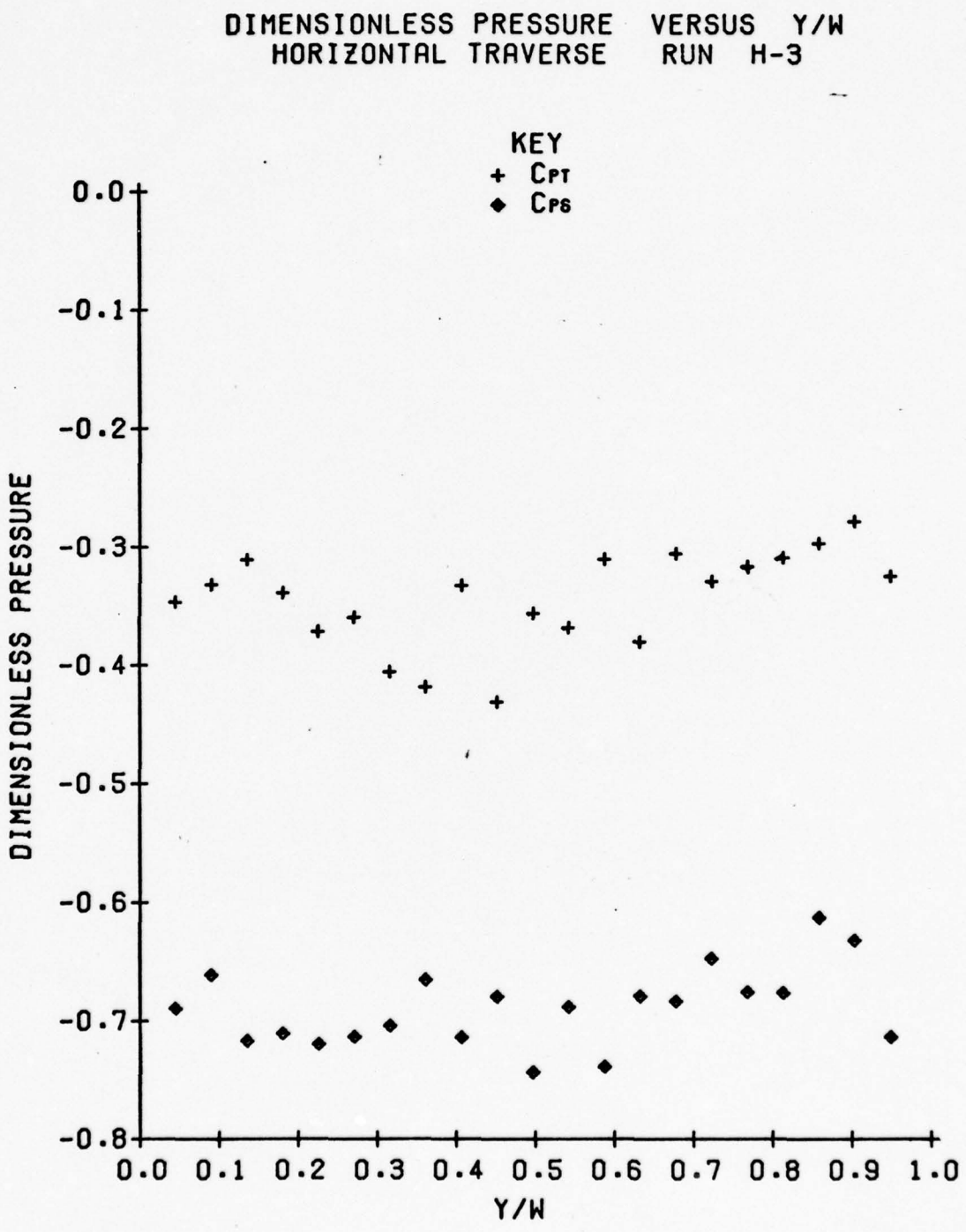

Figure A. 12 Data taken at the volute inlet.

Appendix B

Data taken in the test section
(Simulating the Impeller Eye)

February 8, 1977
AY:tms

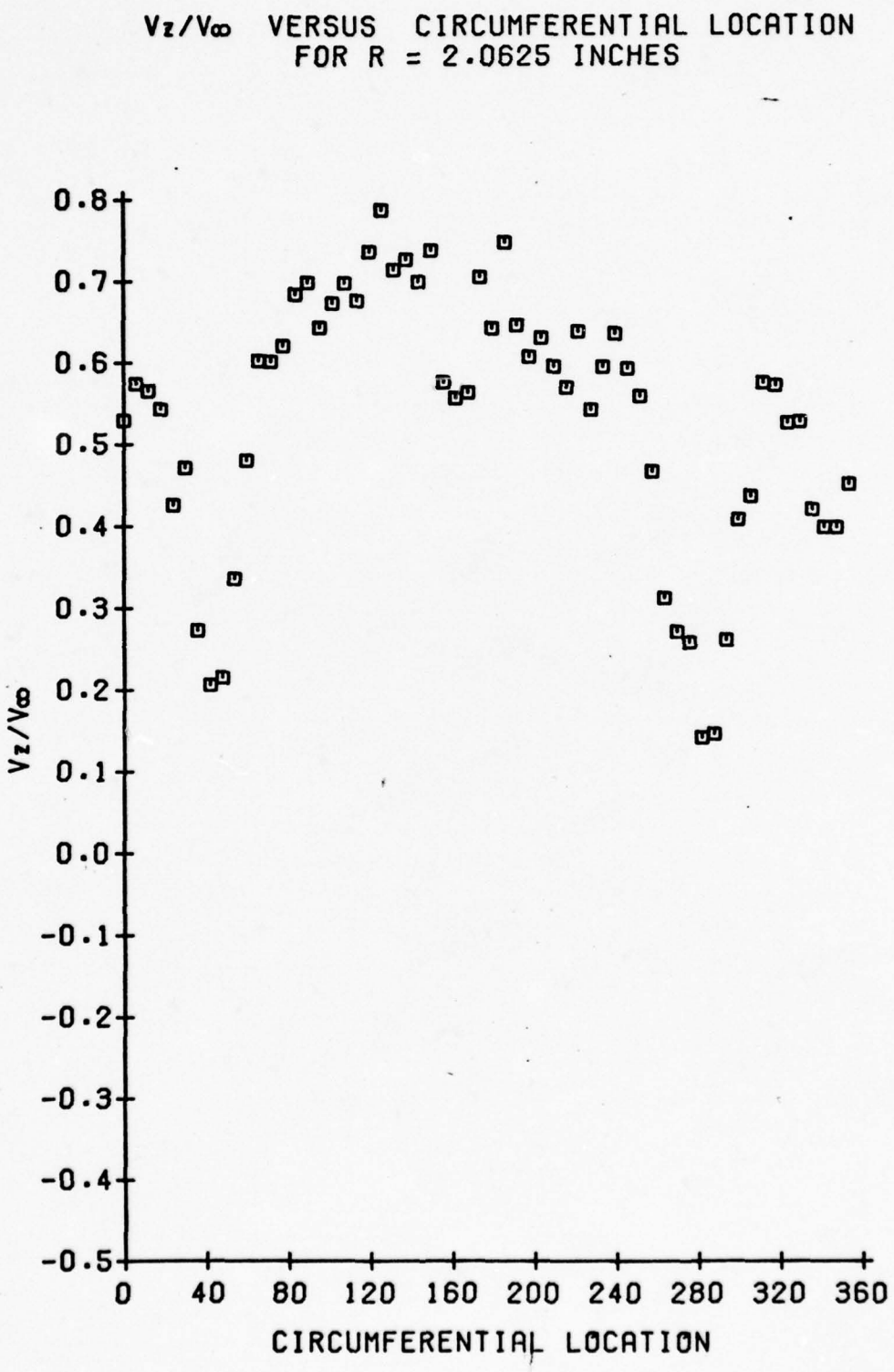

Figure B.1 Data taken in the test section.

February 8, 1977
AY:tms

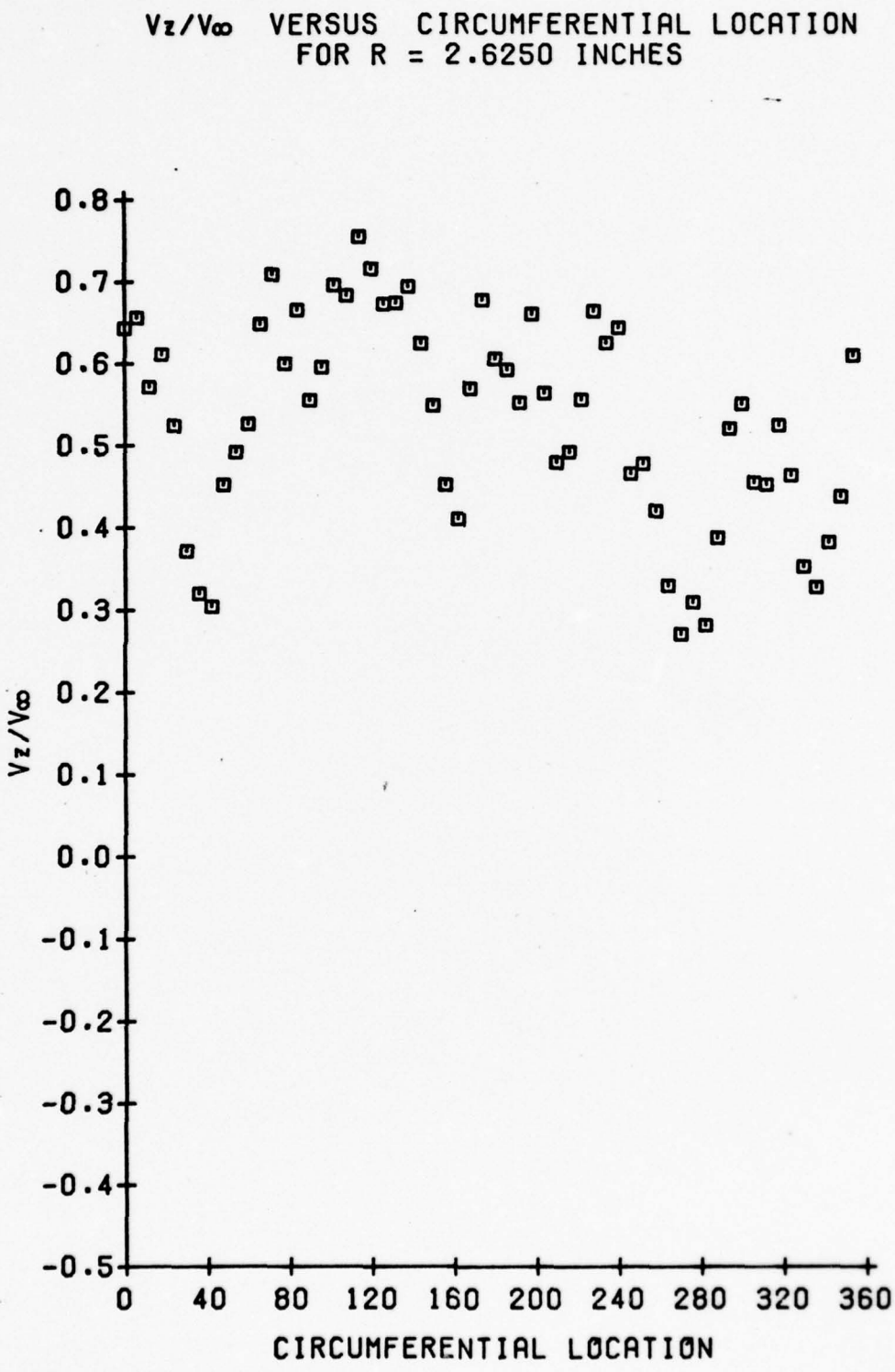

Figure B.2 Data taken in the test section.

February 8, 1977
AY:tms

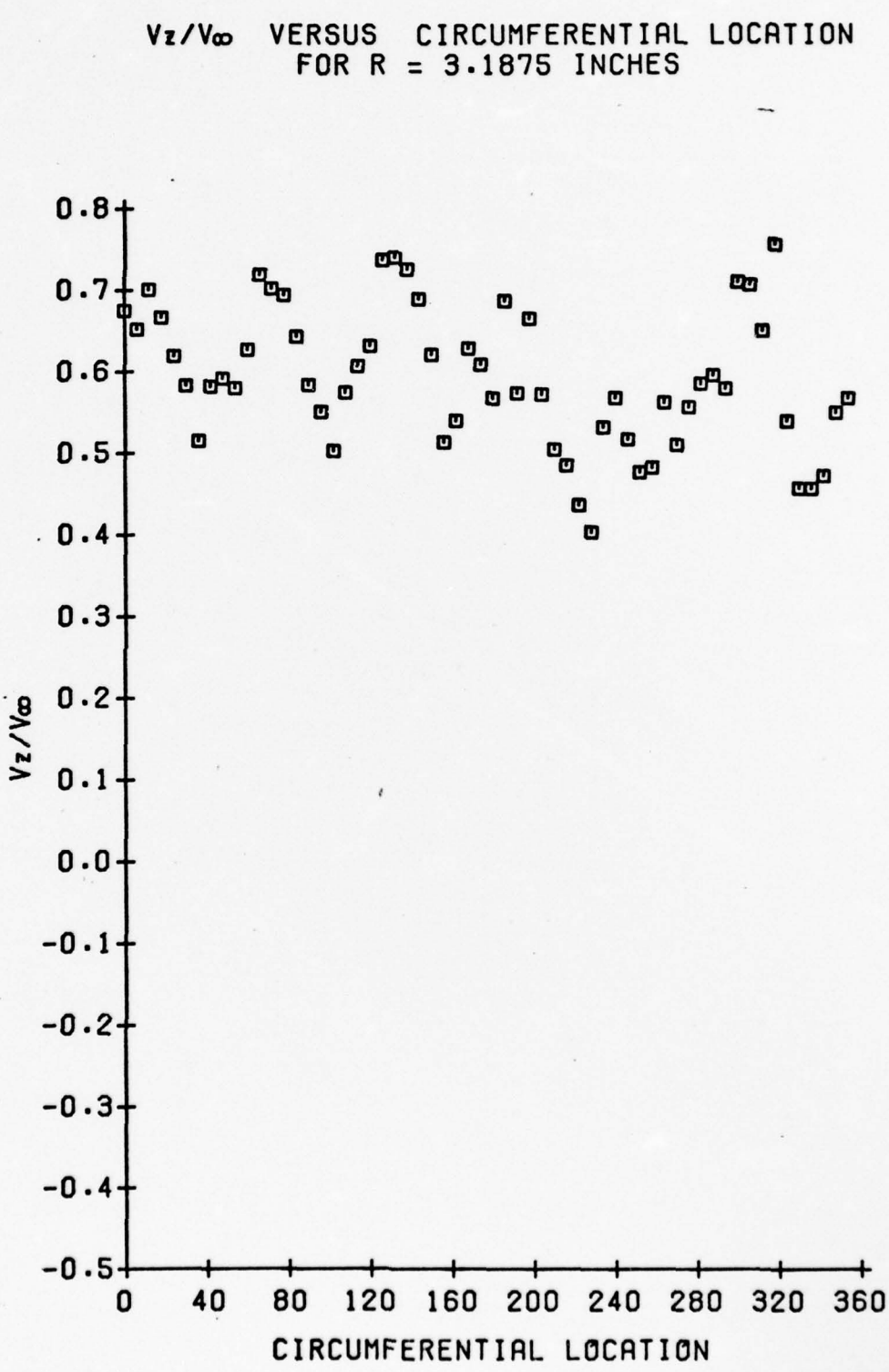

Figure B.3 Data taken in the test section.

February 8, 1977
AY:tms

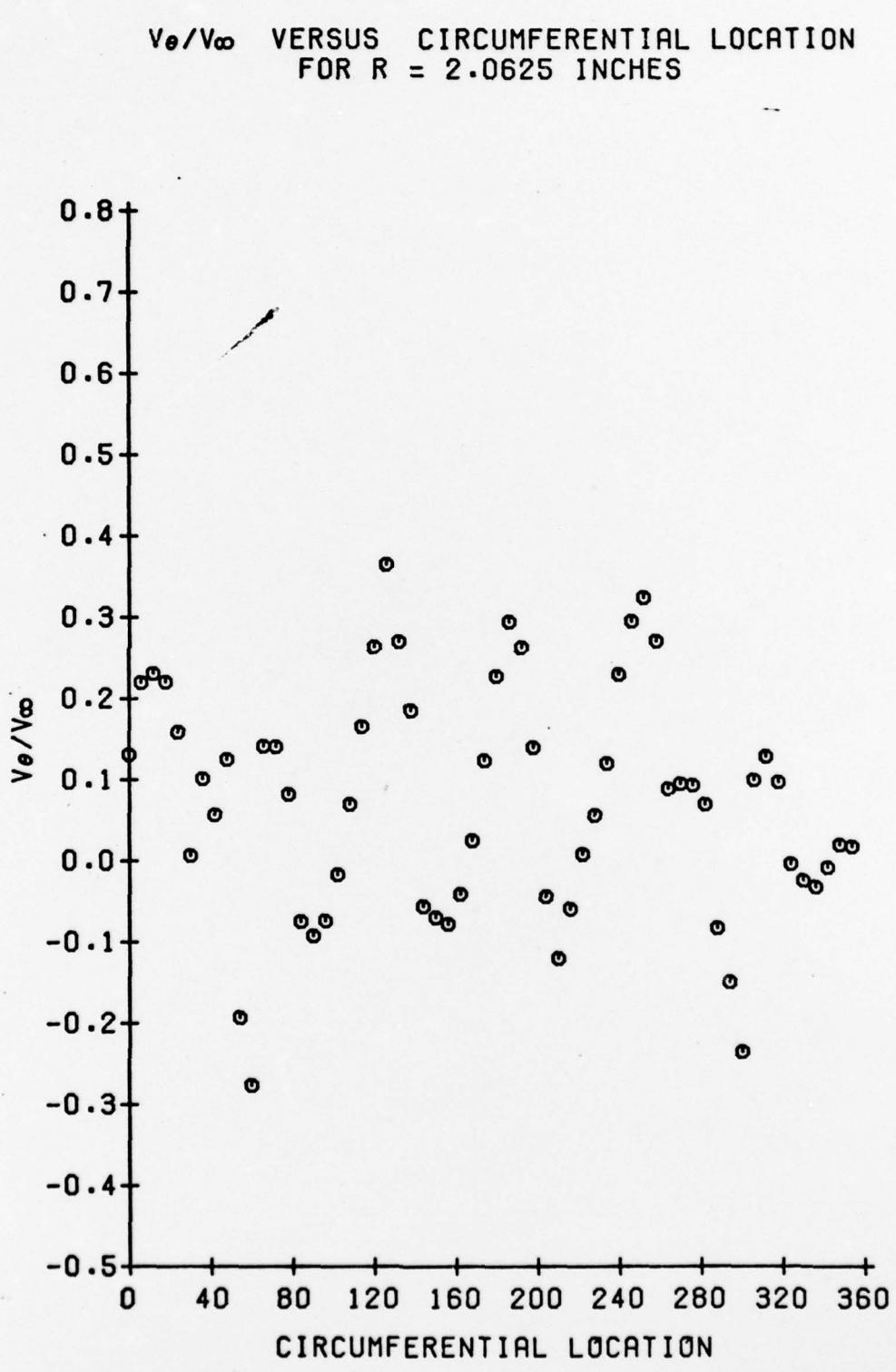

Figure B.4 Data taken in the test section.

February 8, 1977
AY:tms

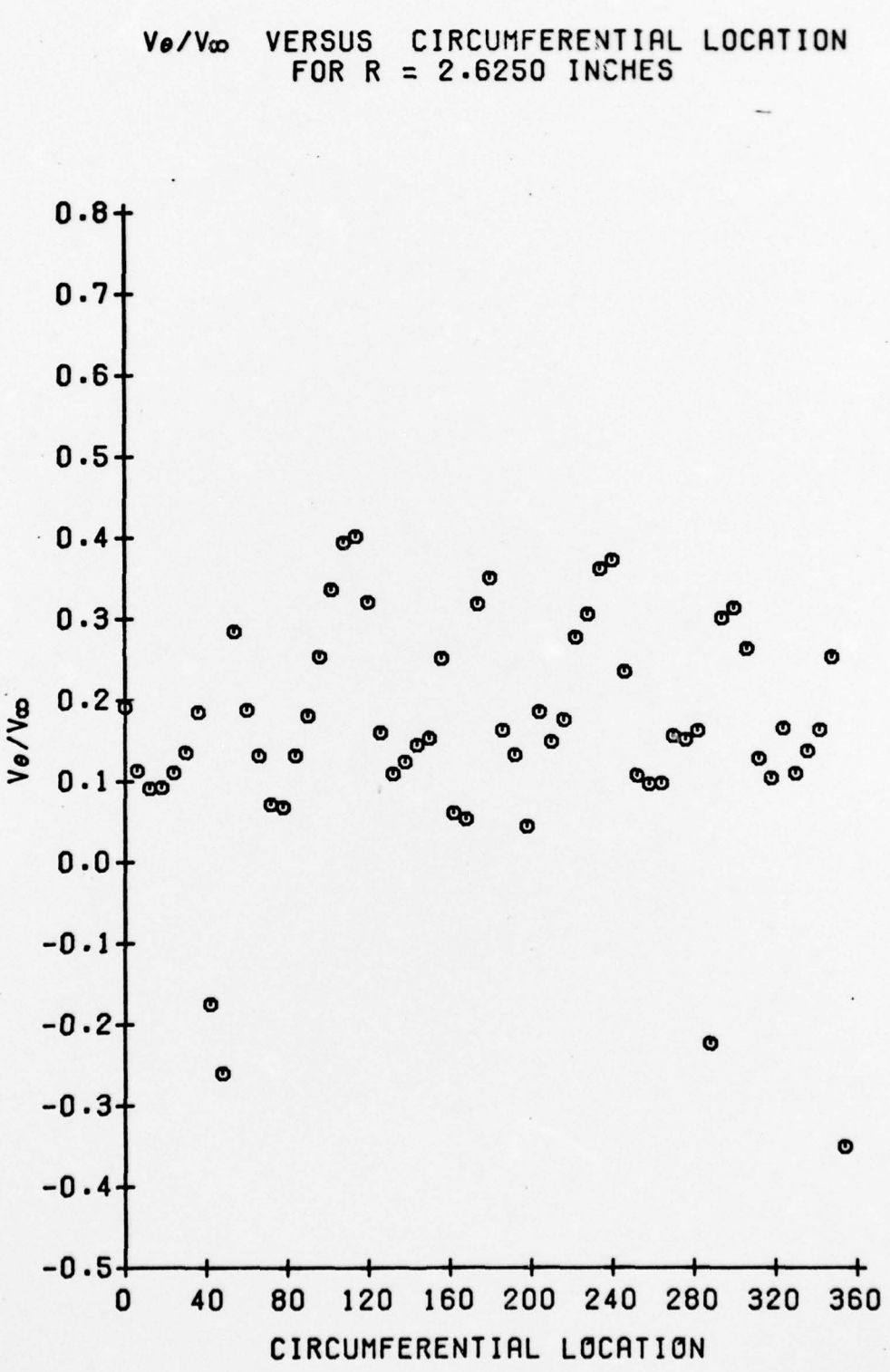

Figure B.5 Data taken in the test section.

February 8, 1977
AY:tms

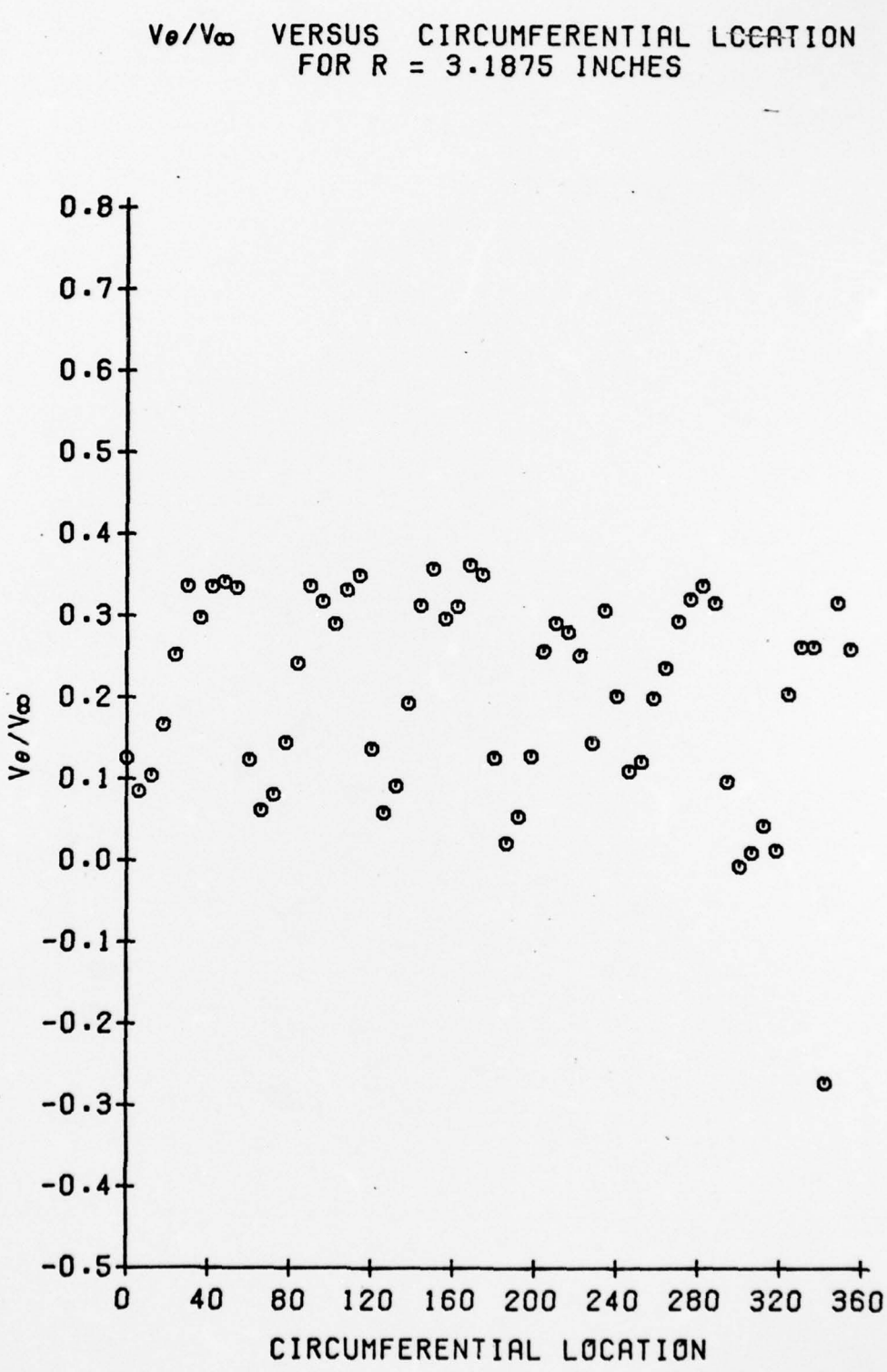

Figure B.6 Data taken in the test section.

February 8, 1977
AY:tms

V_R/V_∞ VERSUS CIRCUMFERENTIAL LOCATION
FOR R = 2.0625 INCHES

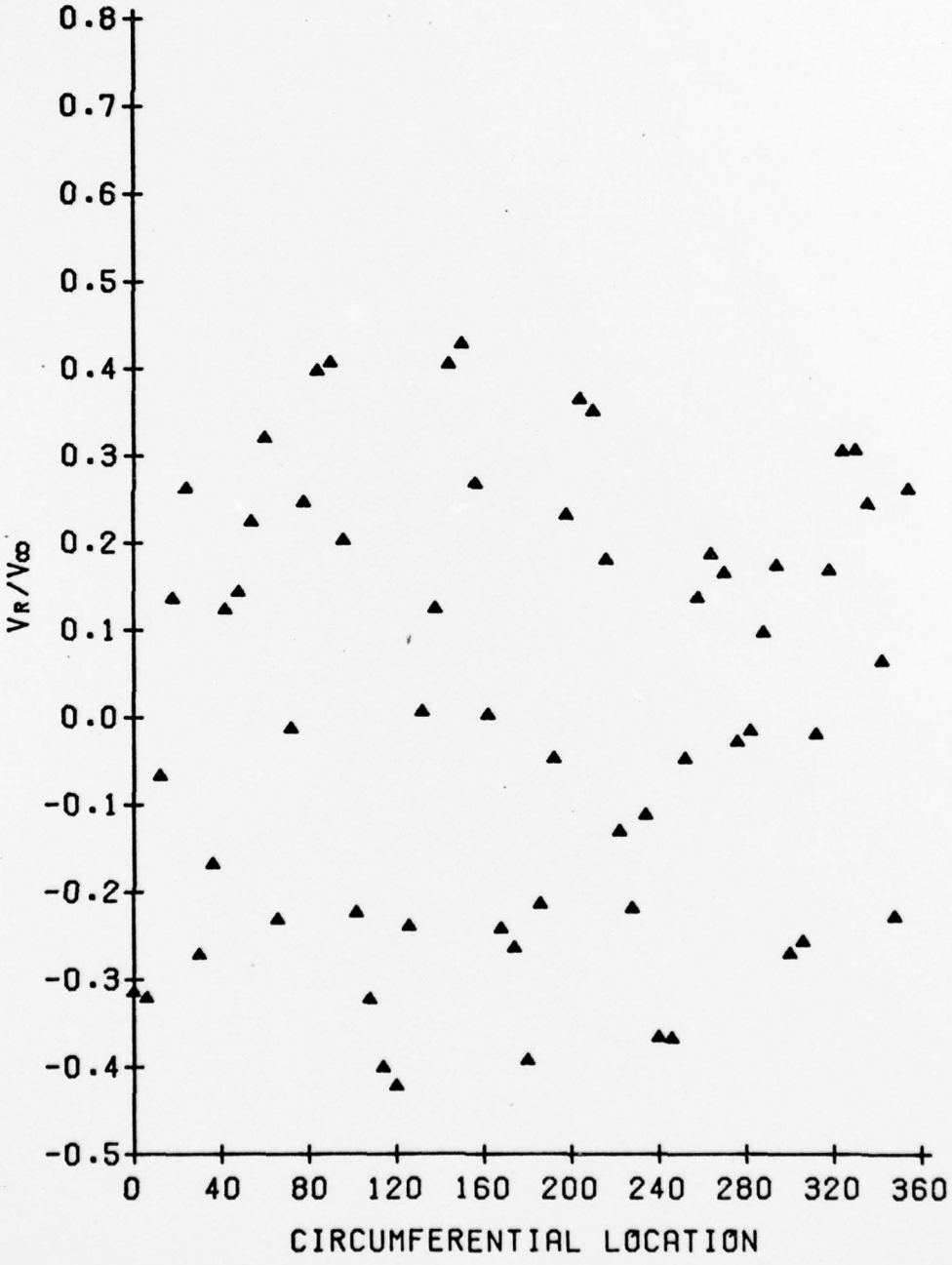

Figure B.7 Data taken in the test section.

February 8, 1977
AY:tms

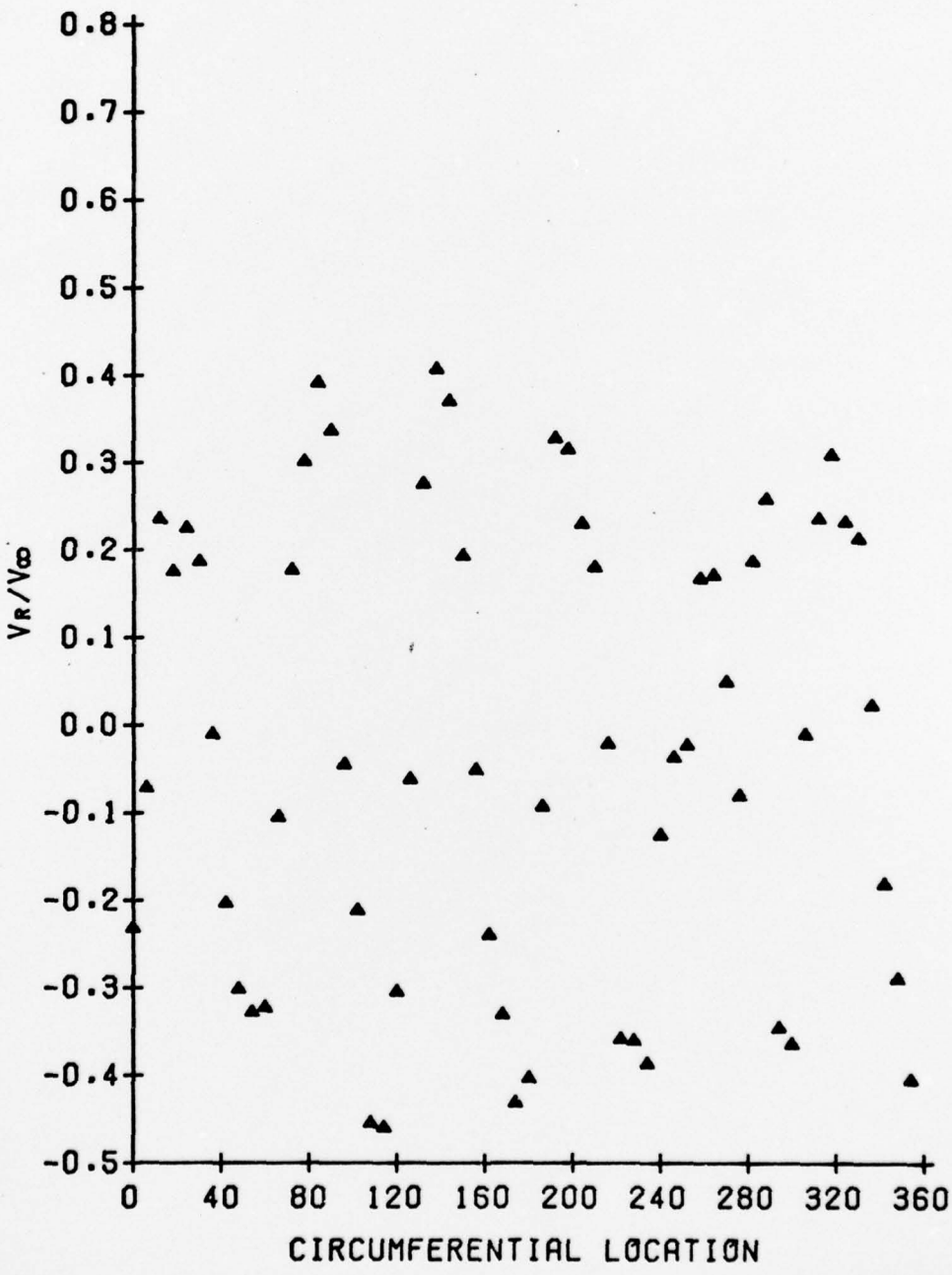

Figure B.8 Data taken in the test section.

February 8, 1977
AY:tms

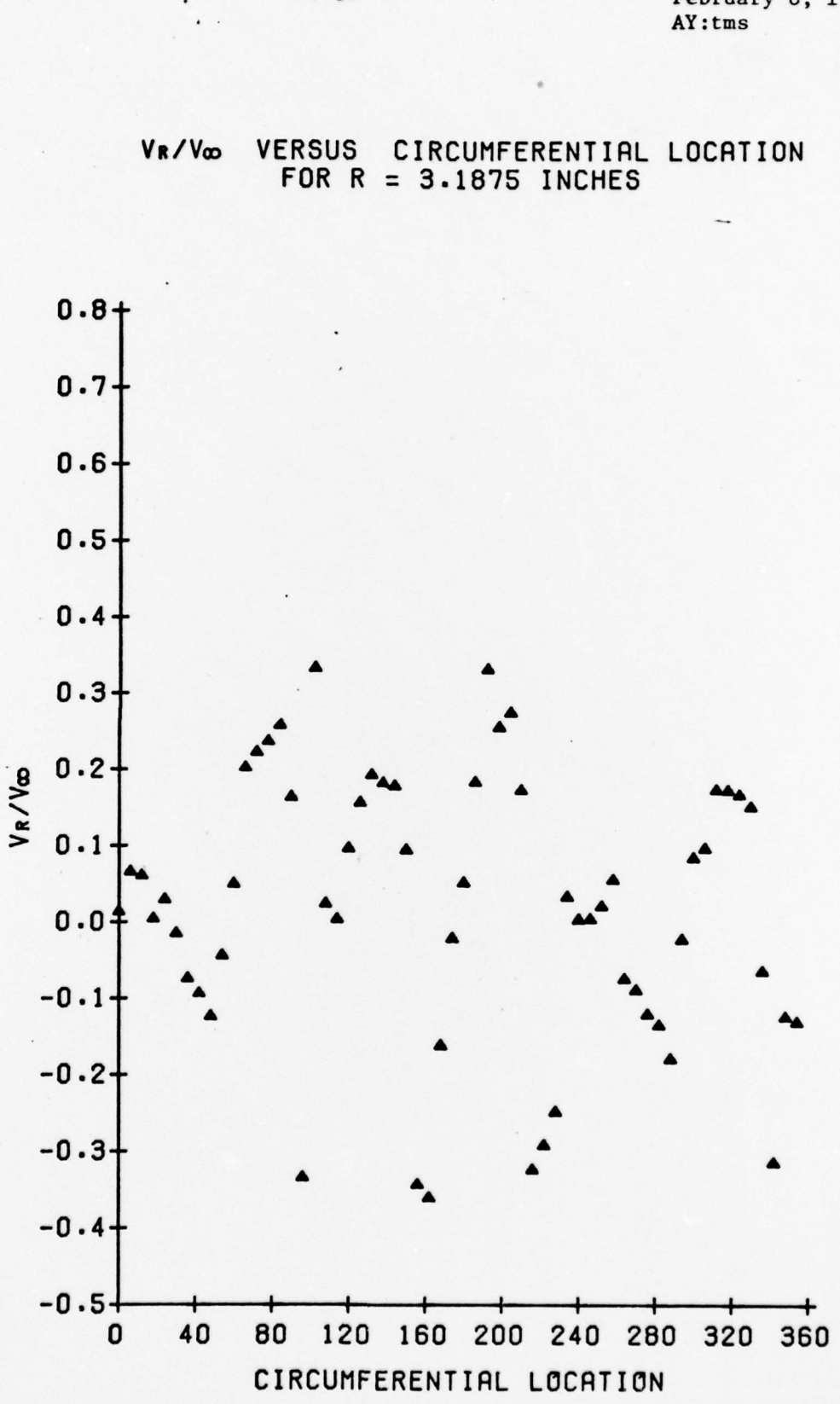

Figure B.9 Data taken in the test section.

February 8, 1977
AY:tms

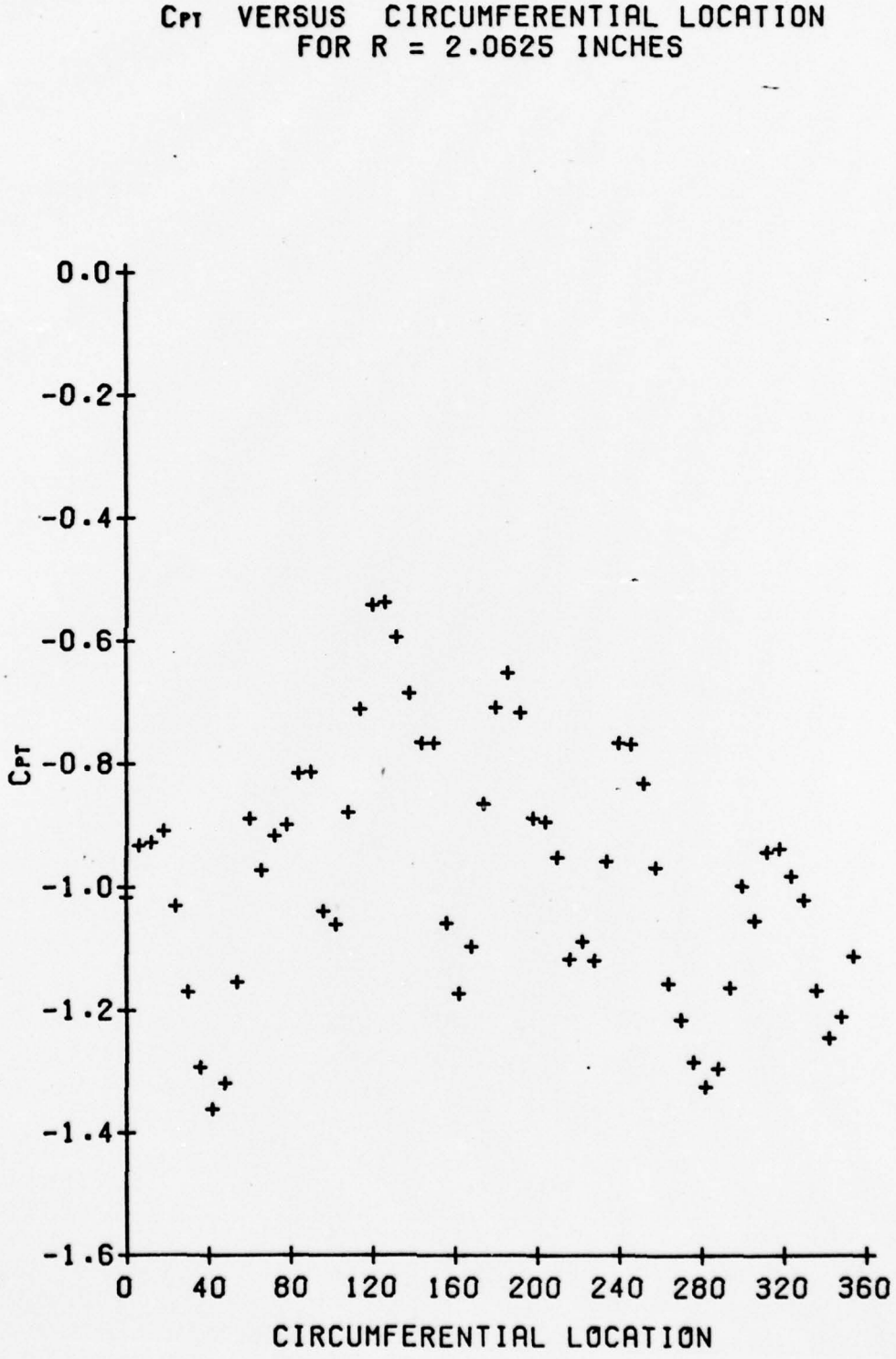

Figure B.10 Data taken in the test section.

February 8, 1977
AY:tms

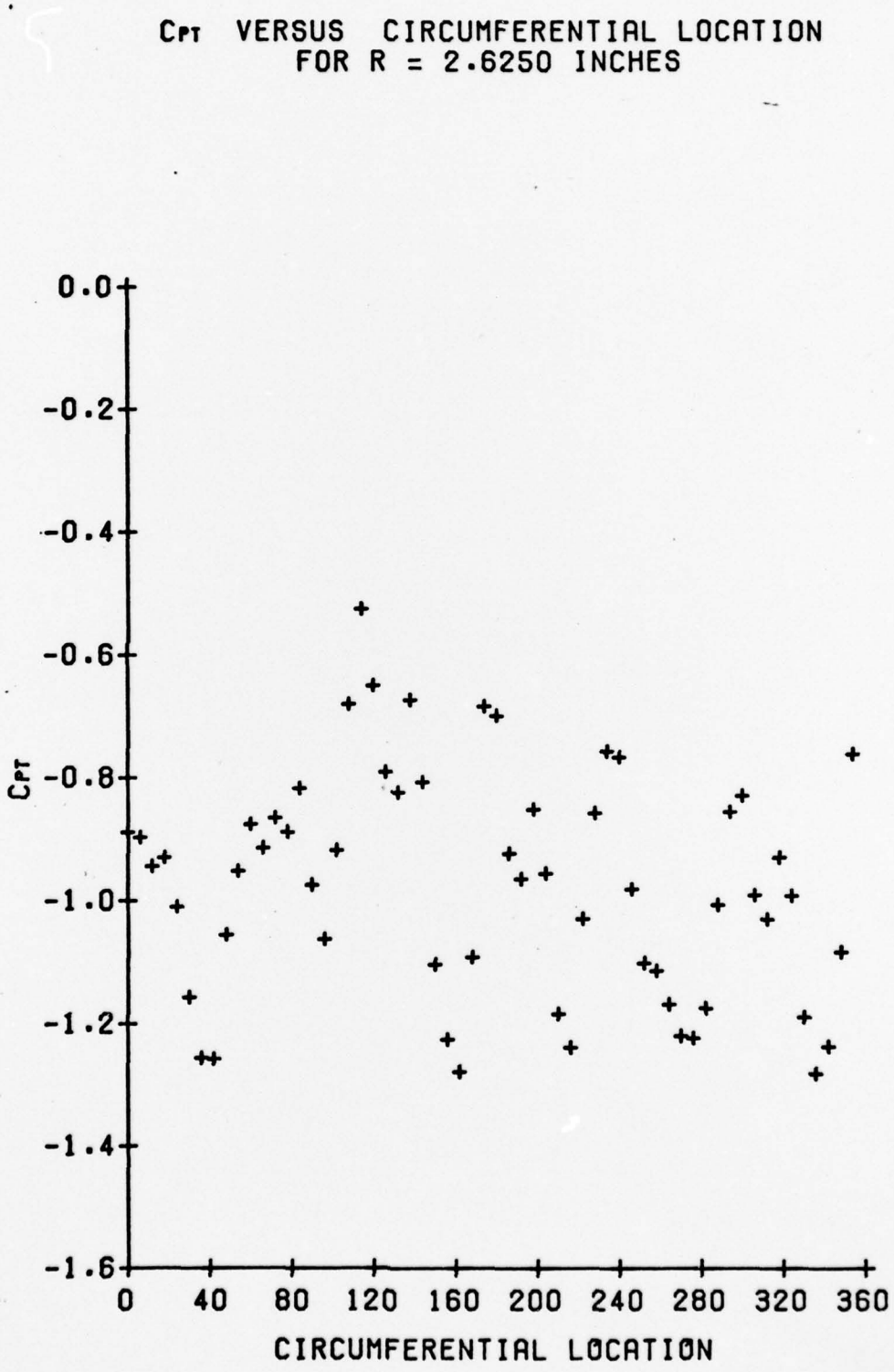

Figure B.11 Data taken in the test section.

February 8, 1977
AY:tms

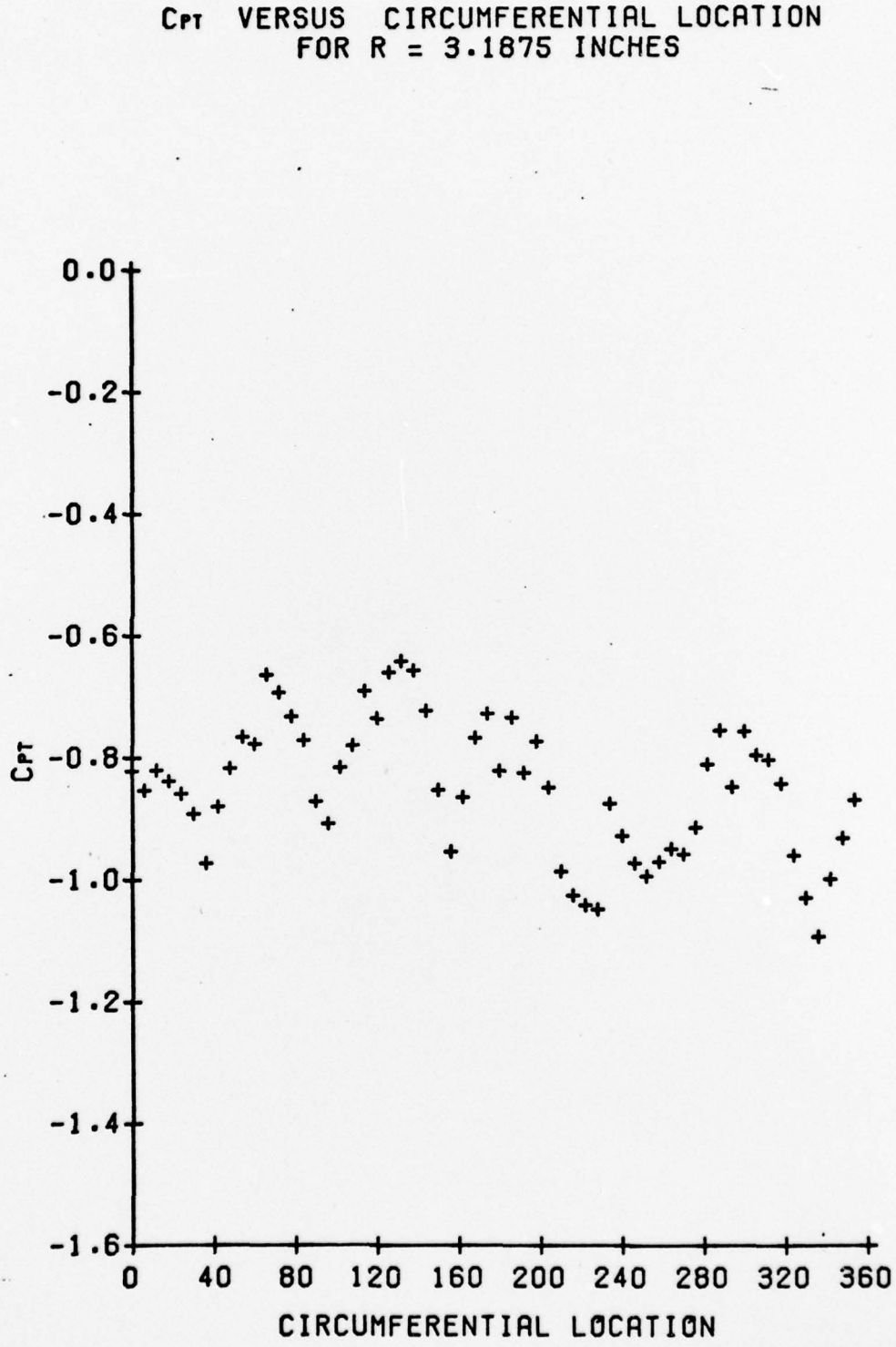

Figure B.12 Data taken in the test section.

February 8, 1977
AY:tms

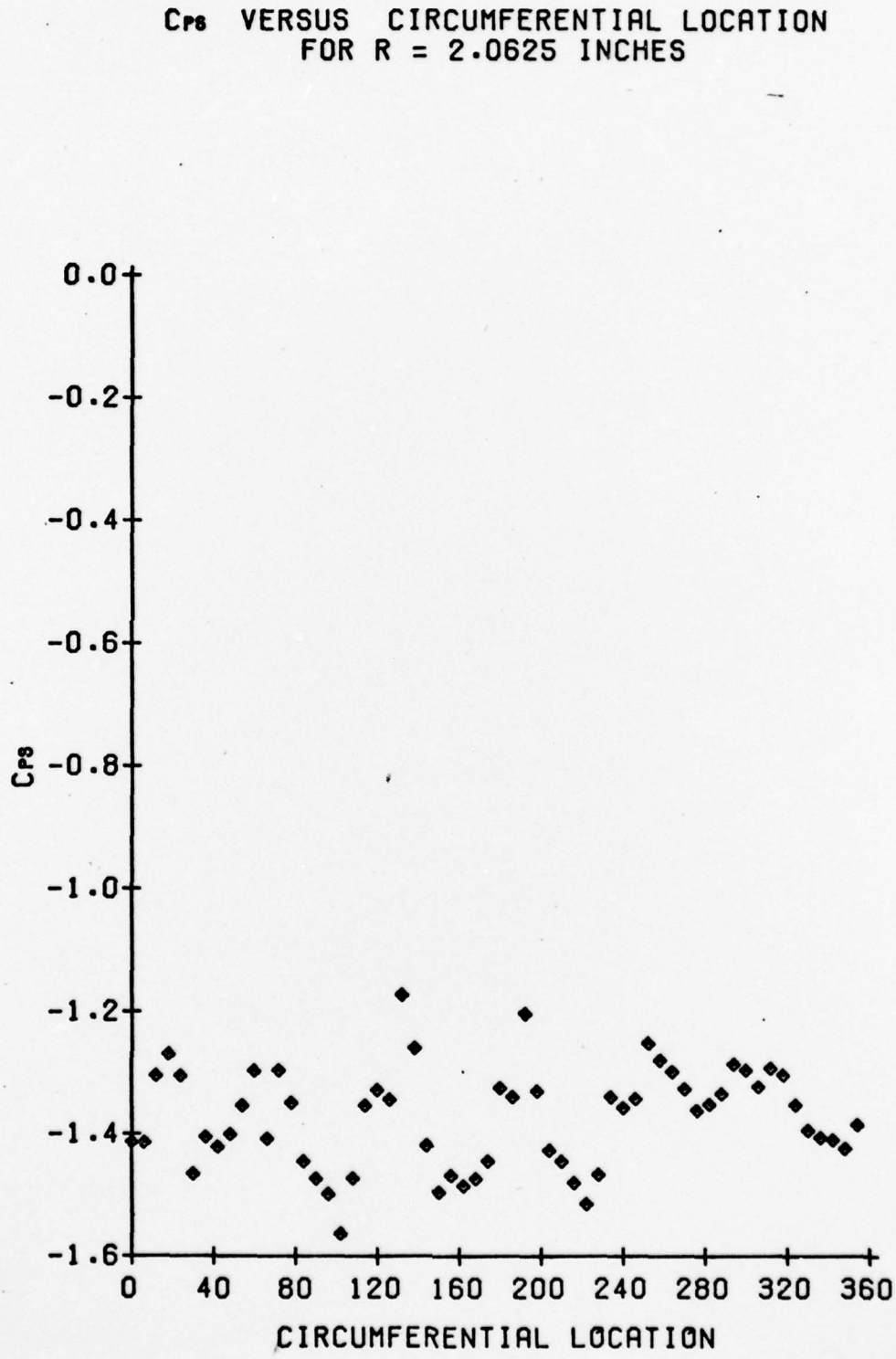

Figure B.13 Data taken in the test section.

February 8, 1977
AY:tms

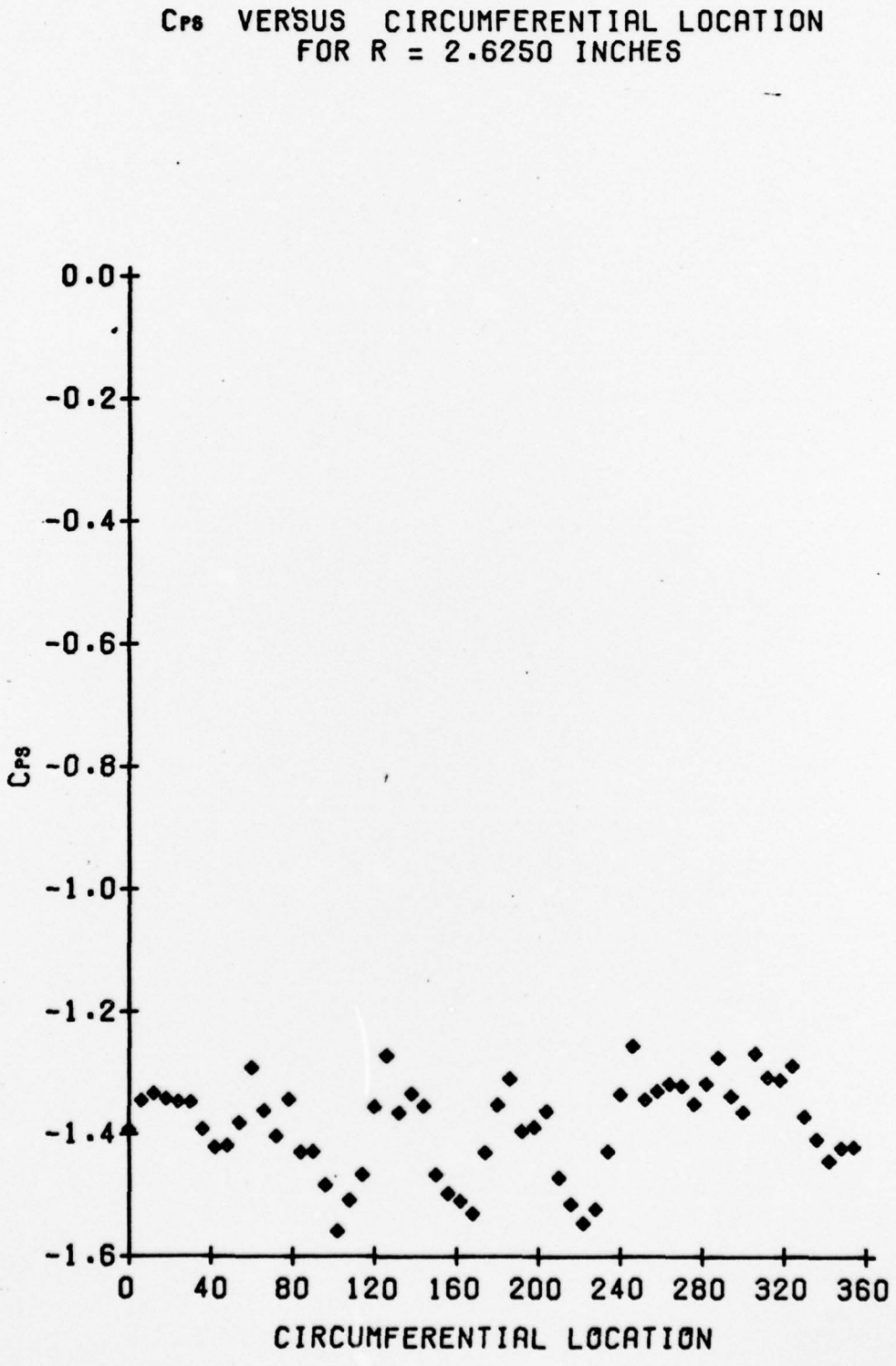

Figure B.14 Data taken in the test section.

February 8, 1977
AY:tms

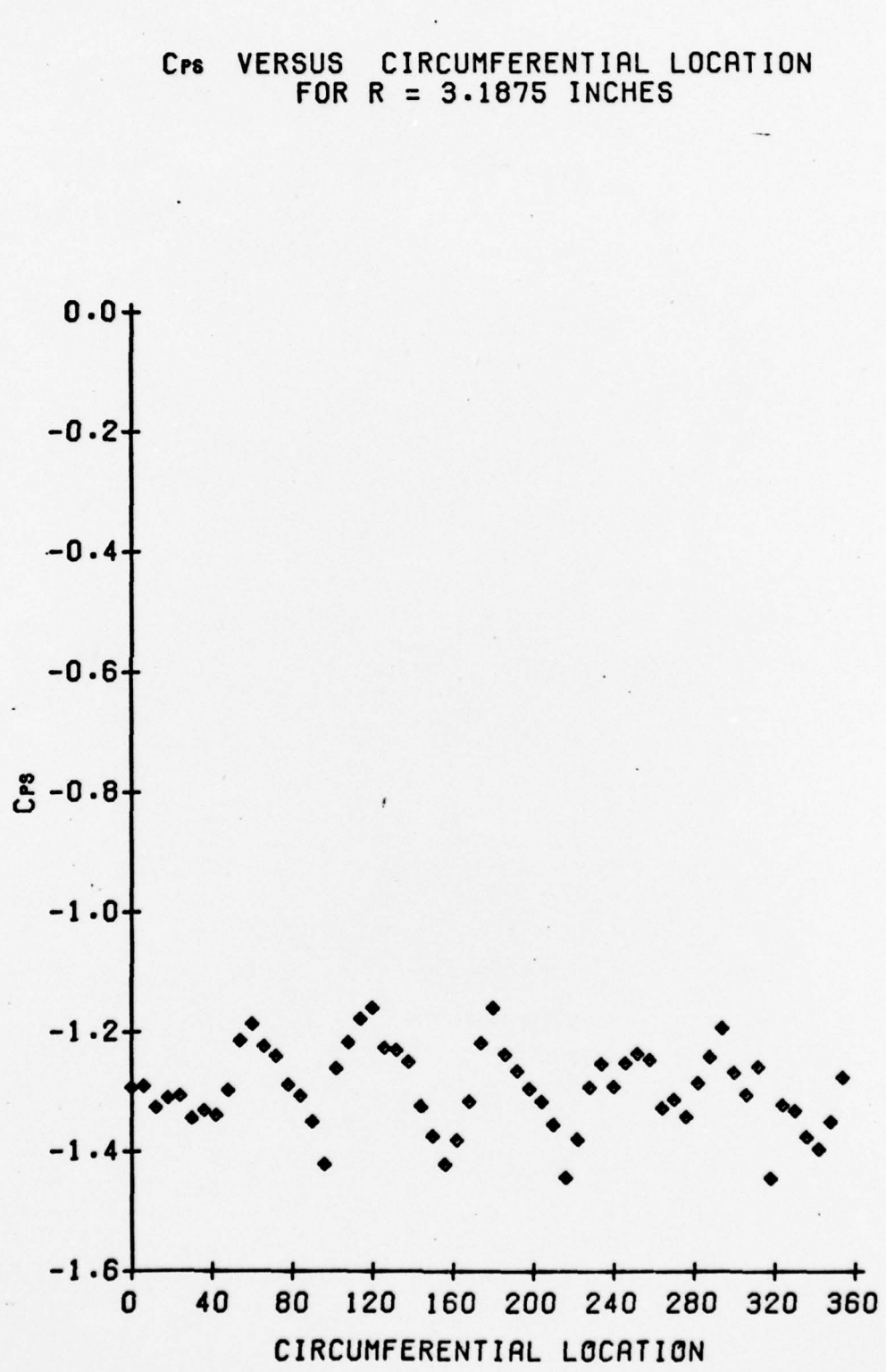

Figure B.15 Data taken in the test section.

DISTRIBUTION LIST FOR UNCLASSIFIED TM 77-34
by A. Yocum (dated February 8, 1977)

Commander
Naval Sea Systems Command
Department of the Navy
Washington, D. C. 20362
Attn: Library
Code SEA-09G32
(Copies 1 and 2)

Naval Sea Systems Command
Attn: S. R. Marcus
Code ORD-03A
(Copy No. 3)

Naval Sea Systems Command
Attn: T. E. Peirce
Code SEA - 0351
(Copy No. 4)

Naval Sea Systems Command
Attn: Code PMS-402
(Copy No. 5)

Naval Sea Systems Command
Attn: G. R. Moltrup
Code SEA - 54
(Copy No. 6)

Naval Sea Systems Command
Attn: Chief Analyst, J. J. Bellaschi
Code SEA - 54
(Copy No. 7)

Naval Sea Systems Command
Attn: C. Miller
Code SEA - 0331G
(Copy No. 8)

Commander
Naval Sea Systems Command
Department of the Navy
Washington, D. C. 20362
Attn: A. R. Paladino
SEA -037
(Copy No. 9)

Naval Sea Systems Command
Attn: L. Benen
Code 03411
(Copy No. 10)

Commander
Naval Ship Engineering Center
Department of the Navy
Washington, D. C. 20360
Attn: W. L. Louis
Code 6136B
(Copy No. 11)

Naval Ship Engineering Center
Attn: R. M. Petros
Code 6148
(Copy No. 12)

Naval Ship Engineering Center
Attn: P. V. Lombardi
Code 6144E
(Copy No. 13)

Naval Ship Engineering Center
Attn: J. R. Buck
Code 6136
(Copy No. 14)

Naval Ship Engineering Center
Attn: M. Hayes
Code 6110.10
(Copy No. 15)

Commanding Officer
Naval Undersea Center
San Diego, CA 92132
Attn: J. W. Hoyt
Code 2501
(Code No. 16)

Naval Undersea Center
Attn: J. Green
Code 254
(Copy No. 17)

Commander Naval Surface Weapon Center
Silver Spring, Maryland 20910
Attn: Library
(Copy No. 18)

Commanding Officer & Director
Naval Ship Res. & Dev. Center
Department of the Navy
Bethesda, Maryland 20084
Attn: W. B. Morgan
Code 154
(Copy No. 19)

DISTRIBUTION LIST FOR UNCLASSIFIED TM 77-34 (Cont'd)

Naval Ship Res. & Dev. Center
Attn: J. B. Hadler
Code 520
(Copy No. 20)

Naval Ship Res. & Dev. Center
Attn: M. Sevik
Code 019
(Copy No. 21)

Naval Ship Res. & Dev. Center
Attn: O. K. Ritter
Code 117
(Code No. 22)

Naval Ship Res. & Dev. Center
Attn: G. F. Dobay
Code 1532
(Copies 23 & 24)

Naval Ship Res. & Dev. Center
Annapolis Laboratory
Annapolis, Maryland 21402
Attn: J. G. Stricker
Code 2721
(Copies 25-28)

Mr. George Wong
Rockedyne Div. Rockwell International
6633 Canoga Avenue
Canoga Park, CA 91304
(Copy No. 29)

Defense Documentation Center
5010 Duke Street
Cameron Street
Alexandria, VA 22314
(Copies 30-41)

Mr. Walter G. Gearhart
APPLIED RESEARCH LABORATORY
The Pennsylvania State University
P. O. Box 30
State College, PA 16801
(Copy No. 42)

Dr. Robert E. Henderson
APPLIED RESEARCH LABORATORY
The Pennsylvania State University
P. O. Box 30
State College, PA 16801
(Copy No. 43)

Mr. Adam Yocum
APPLIED RESEARCH LABORATORY
The Pennsylvania State University
P. O. Box 30
State College, PA 16801
(Copy No. 44)